THE ROLE OF BIOMINERALS IN ENHANCING THE GEOPHYSICAL RESPONSE AT HYDROCARBON CONTAMINATED SITES

By

FARAG MOHAMED MEWAFY

Bachelor of Science in Geophysics
Assiut University
Assiut, Egypt
2000

Master of Science in Geophysics
Assiut University
Assiut, Egypt
2007

Submitted to the Faculty of the Arts and Science
Graduate College of the Arts and Science
Oklahoma State University
in partial fulfillment of
the requirements for
the Degree of Geology
DOCTOR OF PHILOSOPHY
May, 2013

THE ROLE OF BIOMINERALS IN ENHANCING THE GEOPHYSICAL RESPONSE AT HYDROCARBON CONTAMINATED SITES

Dissertation Approved:

Dr. Estella Atekwana

Dissertation Adviser

Dr. James Puckette

Dr. Priyank Jaiswal

Dr. Daniel A. Laó Dávila

Dr. Babu Fathepure

ACKNOWLEDGEMENTS

I would like to sincerely express my immense gratitude to Dr. Estella Atekwana for her tremendous support and encouragement. She was so patient during this long trip. I am so grateful for the time and effort that she devoted as I could not have accomplished this achievement without her sincere support and smart mentorship.

I acknowledge the US Environmental Protection Agency Student Services Contract (EP-10-D-000488). Also, I would like to thank Dr. Dale Werkema for his support and the unique opportunity to work on the EPA student contract.

I would like to thank Dr. Eliot Atekwana, Dr. Lee Slater, Dr. Andre Revil and Dr. Gamal Abdel Aal for their help and guidance during the field and lab work and their help during my writing.

I would like thank my committee members Dr. James Puckette, Dr. Priyank Jaiswal, Dr. Daniel A. Laó Dávila and Dr. Babu Fathepure for their fruitful ideas and guidance during this long trip.

I do also thank the Family of Boone Pickens School of Geology including Alumni, Faculty, Staff and students for making the department a place for success.

Also, my own parents, my brothers and sisters deserve my deepest gratitude. They have all shared my dream and purpose and have constantly been there to help me.

The biggest thank you that comes at the end means something special and this is to the nearest person to my heart “Mona” and her twin “Aisha” who sacrificed their lives for me.

Farag Mewafy

Name: FARAG MEWAFY

Date of Degree: MAY, 2013

Title of Study: THE ROLE OF BIOMINERALS IN ENHANCING THE GEOPHYSICAL RESPONSE AT HYDROCARBON CONTAMINATED SITES

Major Field: GEOLOGY

Abstract: There are several source mechanisms by which microbial activity in the subsurface can change geophysical signatures. To date the source mechanisms generating the geophysical signatures in microbially active environments remain poorly understood. In this study, we investigated the link between the biogeochemical processes resulting in biotransformation of metallic iron mineral phases and the associated biogeophysical signatures. Hydrocarbon contaminated environments provide excellent laboratories for investigating iron mineral biotransformation. In particular, we investigated the magnetic susceptibility (MS) and the complex conductivity (CC) signatures of a hydrocarbon contaminated site near Bemidji, Minnesota.

For the MS study, we investigated the changes in the MS response for cores retrieved from the site as well as down boreholes. The contaminated location revealed two enriched MS zones. The first MS lies within the hydrocarbon smear zone, which is limited to the zone of water table fluctuation with high concentrations of dissolved Fe(II) and organic carbon content. Magnetite and siderite were the dominant minerals formed during this process. However, magnetite was responsible for the bulk of MS changes. The second zone of MS enhancement lies within the vadose zone which is characterized by methane depletion suggesting that aerobic or anaerobic oxidation of methane is coupled to iron-reduction resulting in magnetite precipitation.

For the CC work, we conducted laboratory CC measurements along four cores in addition to field CC survey. We found that the real (σ') and imaginary (σ'') conductivity are higher for samples from within the oil plume especially within the smear zone compared to background uncontaminated samples. Using magnetite as an example of the biometallic minerals in the smear zone at the site, a clear increase in the σ'' response with increasing magnetite content was observed suggesting that the presence of bio-metallic mineral phases as well as electroactive Fe(II) within the smear zone impacts the imaginary conductivity.

Our results suggest that the biogeochemical processes leading to the precipitation of metallic iron mineral phases impacts the geophysical signatures at hydrocarbon contaminated sites undergoing active biodegradation. These bio-metallic minerals (e.g., magnetite) provide us with another source mechanism which has not been considered in previous studies. Therefore, the recognition of the zone of enriched bio-metallic iron mineral phases within the water table fluctuating zone calls for a reevaluation of biogeophysical signatures observed at hydrocarbon contaminated sites commonly attributed to an enhancement of pore water conductivity related to the production of metabolic byproducts.

PUBLICATION DISSERTATION OPTION

This dissertation is organized in two sections. The first section gives an outline of the dissertation and introduces the scientific problem investigated in this study. This section also presents three manuscripts either published or in review for publication. Paper 1, "Magnetic susceptibility as a proxy for investigating microbially-mediated iron reduction" is published in Geophysical Research Letters (2011), focused on investigating if magnetic susceptibility can be used as an intrinsic bioremediation indicator due to the activity of iron-reducing bacteria. Paper 2, "Evidence that biometallic mineral precipitation enhances the complex conductivity response at a hydrocarbon contaminated site" (in review in the Journal of Applied Geophysics) focuses on elucidating the major factors controlling the complex conductivity response at hydrocarbon contaminated sites undergoing biodegradation. Paper 3, "High-resolution magnetic susceptibility measurements for investigating magnetic mineral formation during microbial mediated iron reduction" investigates the hydrobiogeochemical factors controlling variations in magnetic susceptibility across a hydrocarbon contaminated site undergoing biodegradation where iron reduction and methanogenesis are the main terminal electron acceptor processes. This work is being prepared for publication. The second section summarizes the major conclusions of the work.

TABLE OF CONTENTS

LIST OF FIGURES

SECTION 1

GENERAL OVERVIEW

1.0. MOTIVATION

Microbes are the most abundant and most diverse forms of life on earth (Whitman et al., 1998). In the subsurface, microbes are known to alter geologic media through the process of biomineralization, the formation of biofilms, and the production of metabolic byproducts that change the physicochemical properties of the media (see Atekwana et al., 2006 for extensive review). The bio-induced physicochemical changes of porous media by microbial activity generate measurable geophysical signatures (Atekwana and Slater, 2009). Over the last decade, significant advances in the field of near-surface geophysics, and biogeophysics in particular have established a link with geophysical response to microbial growth and enzymatic activity in geologic media especially for contaminated sites. However, the interpretation of the geophysical data remains speculative because many mechanistic aspects of the relationships between biological interactions with geologic media and the ensuing geophysical properties remain poorly understood. In this study we investigated the complex conductivity (CC) and the magnetic susceptibility (MS) signatures for a hydrocarbon contaminated site near Bemidji, Minnesota. We

observed that the bio-metallic minerals have greater impacts on the CC and the MS response and should be considered in the interpretation of geophysical data from contaminated sites.

1.1. PRESENT STATE OF KNOWLEDGE

The presence of organic contaminants in the subsurface (e.g., hydrocarbons) stimulates biological activity, resulting in bio-physicochemical changes induced in the subsurface during the biodegradation of hydrocarbons by microbes (Cozzarelli et al., 1994; Cozzarelli et al., 2001; Cassidy et al., 2002). Figure (1) is a schematic representation of the important bio-physicochemical changes induced in the subsurface porous media during the biodegradation of hydrocarbons by microbes (Davis et al., 2006). Microorganisms provided with organic carbon and nutrients will increase in cell numbers. The increase in cell numbers on the surfaces of the substrate and between pore openings in rocks and sediments can also induce physical changes (e.g., porosity, permeability, surface area) in the porous material itself (Zywietz and Knochel, 1986; Clement et al., 1996; Thullner et al., 2002; Atekwana and Slater, 2009; Abdel Aal et al., 2010, Atekwana and Atekwana, 2010). Microbial breakdown of hydrocarbon and other organic compounds produce organic and carbonic acids. These acids are in turn responsible for the leaching of the surrounding soil matrix causing an increase in the ionic strength of the pore water (Atekwana et al., 2004b). Hence, the dissolution of minerals results in etching of the grains of the soil matrix (Bennett et al., 1996). These changes may cause an increase in the bulk electrical conductivity of contaminated soil that is detectable by geophysical methods such as complex conductivity (CC) (Abdel Aal et al., 2006), bulk electrical conductivity (Atekwana et al., 2004c), and ground-penetrating radar (Sauck et al., 1998; Cassidy, 2008a; b; Che-Alota et al., 2009). Previous geophysical investigations have documented elevated bulk electrical conductivity at

hydrocarbon contaminated sites resulting in what is commonly referred to as the conductive plume model (Sauck, 2000). Several explanations have been suggested for this enhancement in bulk conductivity. Werkema et al. (2003) attributed the enhancement in bulk electrical conductivity to mineral weathering associated with microbial redox processes and subsequent increase in fluid conductivity. Interestingly, they noticed that changes in water conductivity could not account for the entire enhancement in bulk electrical conductivity. A study by Atekwana et al. (2004b) evaluated the relationship of total dissolved solids (TDS) measurements to bulk electrical conductivity in an aquifer contaminated with hydrocarbons. Their bulk electrical and fluid conductivity data from some contaminated locations showed an inverse relationship at low fluid conductivity (<40 mS/m) and a poor positive relationship for higher fluid conductivity (>40 mS/m). However, none of the previous studies considered the role of precipitated mineral phases, especially conductive minerals in enhancing the geophysical signature at hydrocarbon contaminated sites.

In the redox reaction process, the presence of terminal electron acceptors governs nutrient utilization by microbes during the breakdown of organic carbon (Bekins et al., 2001; Cozzarelli et al., 2001). Terminal electron acceptors are sequentially utilized from O_2, NO_3^-, Fe(III), Mn (IV), SO_2^{-4} and CO_2. Iron(III)-reducing microorganisms can use hydrocarbons as a carbon source to reduce iron(III) to iron(II) (Lovley et al., 1989; Anderson and Lovley, 2000). This coupling process can lead to the formation of ferrous bio-minerals such as magnetite. Biomineralization pathways can be affected by many factors that may include pH, redox potential, carbonate concentration and, mostly, respiration-driven Fe(II) supply rate and magnitude (Fredrickson et al., 1998; Zachara et al., 2002). For instance, Zachara et al. (2002) related the formed iron phase to the Fe(II) supply rate. At lower supply rates, they

observed the precipitation of Fe(III) oxides; while at medium and higher rates, magnetite and siderite were dominant precipitates respectively. In a laboratory experiment by Hansel et al. (2003, 2005) shows that the magnetite can be the end product of a long process of ferrihydrite reduction that goes through ferrous hydroxide ($Fe(OH)_2$) where Fe(II) is dissolved then to green rust and ends with magnetite (Figure 2). Also in the case of high Fe(II) concentration, Fe(II) can be sorbed directly to ferrihydrite to precipitate fine grained magnetite (Hansel et al, 2003).

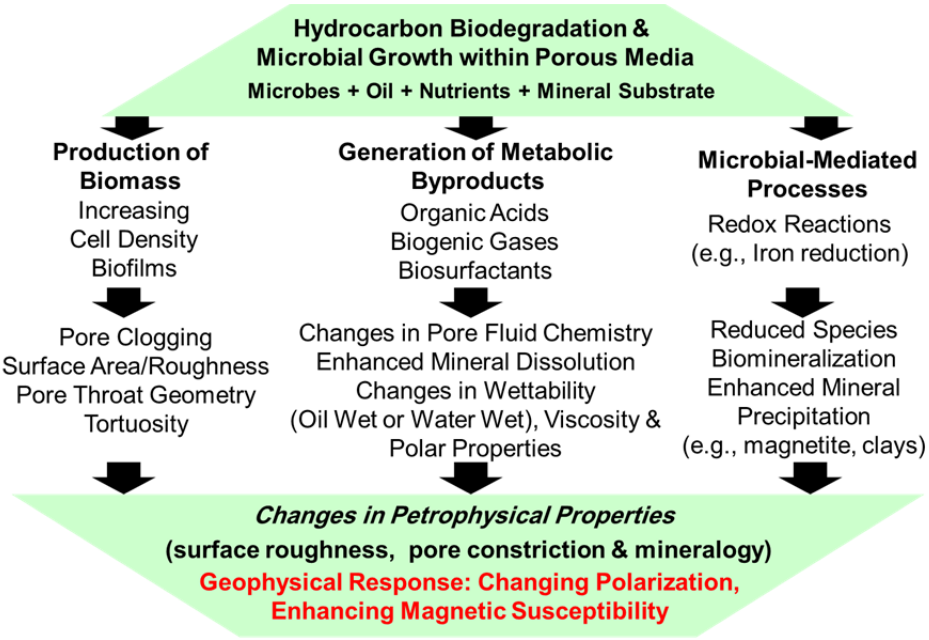

Figure 1. Generalized conceptual diagram showing various pathways by which microorganisms can alter the physicochemical properties, and, thus, potentially the geophysical signatures (modified from *Davis et al.* 2006).

The precipitation of metallic iron biominerals can result in many geophysical responses (Figure 3). Figure 3 is a conceptual model showing how different biomineralization pathways

can result in geophysical responses. Some of these iron phases are conductors such as goethite (Guskos et al., 2002), greigite (Dekkers et al., 2000), and lepidocrocite (Guo and Barnard, 2011) to semiconductors such as pyrite (Karguppikar and Vedeshwar, 1988) and magnetite (Simsa and Brabers, 1988). While other minerals such as siderite (Parkhomenko, 1982) and ferroan calcite (Amabeoku et al., 1995) are poor conductors. As the different iron mineral phases vary in their magnetic and electric properties, the MS and CC signature will vary based on the precipitated iron mineral phase (Figure 3).

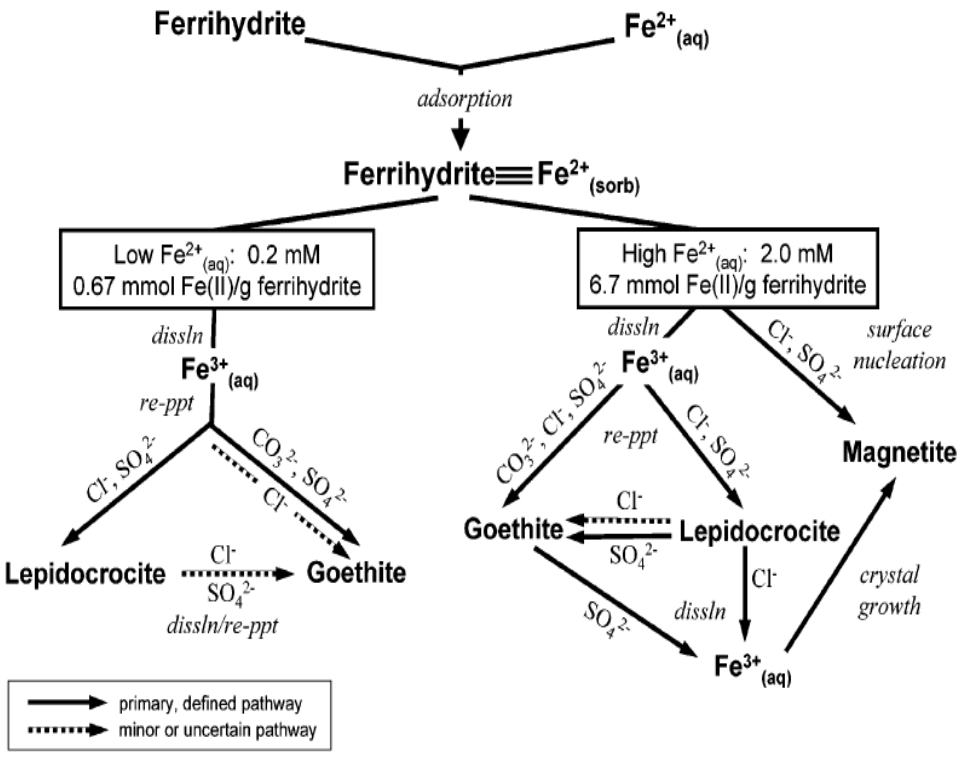

Figure 2. Conceptual model depicting the secondary phase transformation of ferrihydrite as a function of Fe(II) concentration and ligand (circumneutral pH). Dissln = dissolution; re-ppt = reprecipitation (Hansel et al., 2005).

Previous laboratory studies documented a significant impact of metallic biominerals on the CC response due to an enhancement of electrode polarization (e.g., Williams et al., 2005, Slater et al., 2007), however the effect of biometallic biominerals on the CC has not been considered by previous studies in the interpretation of complex conductivity data from oil contaminated sites undergoing intrinsic bioremediation. Recently, Rijal et al. (2010, 2012) showed that the accumulation of metallic biominerals can end with zones of enhanced magnetic minerals which can be detected using magnetic susceptibility (MS). In this study, we investigated the magnetic susceptibility and complex conductivity signatures of a hydrocarbon contaminated site near Bemidji, Minnesota, USA. The main goal of this work is to link the geophysical response to the subsurface hydrobiogeochemical processes in the contaminated aquifer.

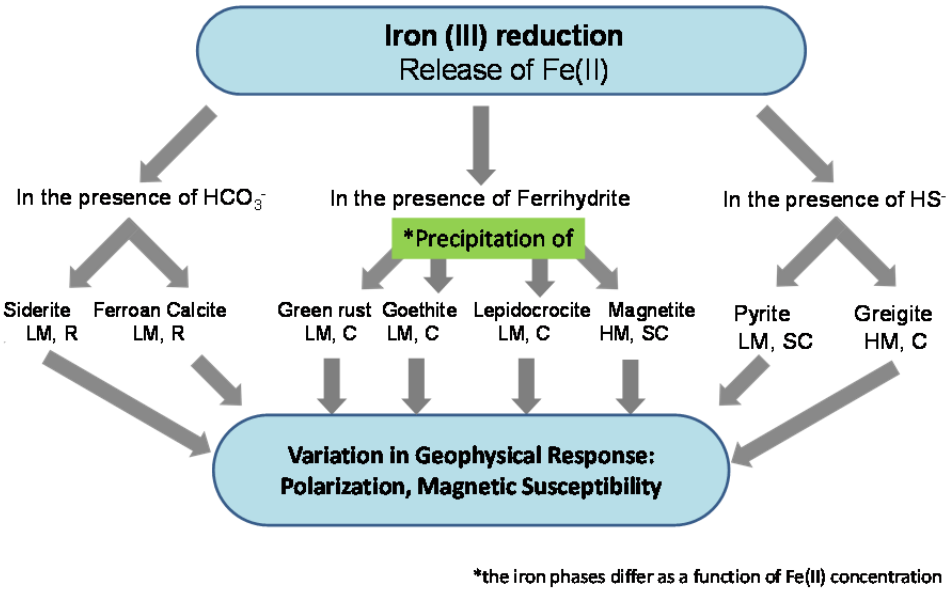

Figure 3. Conceptual model showing different biomineralization pathways that may impact geophysical signatures. Some of these iron phases show low magnetic (LM) or high magnetic (HM) responses. These iron phases vary between resistors (R), semiconductors (SC), and conductors (C).

The contaminated plume within Bemidji site has three main biogeochemical zones (Baedecker et al., 1993; Bennett et al., 1993; Eganhouse et al., 1993). It starts with a distal aerobic zone with low dissolved O_2 that develops gradually to a zone of aromatics oxidation coupled to dissimilatory Mn(III/IV) and Fe(III) reduction (Lovley et al., 1989; Eganhouse et al., 1993; Anderson and Lovley, 1999) and ends with an anoxic zone (includes the smear zone) within the heart of the plume where methanogenesis is dominant. The methanogenesis occurs after the bioavailable Mn(III/IV) and Fe(III) have been depleted from the sediment (Anderson and Lovley, 1999). Cozzarelli et al. (1990) reported an increase in organic acids such as orthotoluic, cyclohexanoic and acetic acids towards the center of the plume. The acetic acid is an indicator that geochemical zone towards the center of the plume turn to methanogensis.

1.2. RESEARCH OBJECTIVES

The goal of the work was to accomplish the following objectives:

1. Document the presence of biogenic minerals (magnetite) using field and laboratory MS measurements
2. Evaluate the contribution of metallic biominerals specifically magnetite to CC signatures,
3. Determine the hydrobiogeochemical controls on the MS variability.

Accomplishing these objectives, through a combination of field and laboratory experiments is expected to help us test the following hypotheses:

Hypothesis 1: ***At a hydrocarbon contaminated site, magnetite enrichment can be an indication of microbially mediated iron reduction coupled with hydrocarbon oxidation.***

Hypothesis 2: ***The presence of bio-induced mineral precipitation enhances the CC response.***

Hypothesis 3: ***Magnetic susceptibility can be used to understand the coupling of organic carbon and iron.***

1.4. PROJECT SIGNIFICANCE

Geophysics can help in the understanding of biogeochemical processes in the subsurface by pointing to specific interfaces where these processes are occurring. Microbial and geochemical sampling of key biogeochemical interfaces guided by geophysical techniques such as CC and MS can provide critical understanding these biogeochemical processes. Linking the CC and the MS responses to the geochemical processes, especially iron cycling, in the subsurface is important for: (1) understanding the coupling of biogeochemical cycles (e.g., coupling of organic carbon and iron cycling), (2) detecting the fate and transport of organic contaminants in the groundwater, (3) guiding geochemists and microbiologists to locate the right targets for subsurface soil and microbial sampling in a cheap, time-effective way, and (4) advancing the technology for oil exploration and soil bioremediation by following iron precipitation related to oil accumulations and/or migration.

1.4. REFERENCES

Abdel Aal, G. Z. A., L. D. Slater, and E. A. Atekwana (2006), Induced-polarization measurements on unconsolidated sediments from a site of active hydrocarbon biodegradation, *Geophysics*, *71*(2), H13-H24.

Abdel Aal, G. Z., E. A. Atekwana, S. Rossbach, and D. D. Werkema (2010), Sensitivity of geoelectrical measurements to the presence of bacteria in porous media, Journal of Geophysical Research, 115, G03017, doi:10.1029/2009JG001279.Allen, J.P., E.A.

Amabeoku, M., K. Mimoune, and S. Al-Nufaili (1995), Lithological variability of electrical parameters in a sandstone sequence, Middle East Oil Show.

Anderson, R.T., and D.R. Lovley (1999), Naphthalene and benzene degradation under Fe(III)-reducing conditions in petroleum-contaminated aquifers. Bioremediation Journal, 3: 121–135.

Anderson, R.T., and D.R. Lovley (2000), Anaerobic bioremediation of benzene under sulfate-reducing conditions in a petroleum-contaminated aquifer. Environ Science and Technology; 34: 2261–2266

Atekwana, E., and E. Atekwana (2010), Geophysical Signatures of Microbial Activity at Hydrocarbon Contaminated Sites: A Review, Surveys in Geophysics, 31(2), 247-283.

Atekwana, E.A., and L.D. Slater (2009), Biogeophysics: A new frontier in earth science research Reviews of Geophysics, 47.

Atekwana, E.A., D.D. Werkema, J.W. Duris, S. Rossbach, W.A. Sauck, D.P. Cassidy, J. Means, and F.D. Legall (2004c), In-situ apparent conductivity measurements and microbial population distribution at a hydrocarbon-contaminated site, Geophysics, 69(1), 56-63.

Atekwana, E.A., E. Atekwana, F.D. Legall, and R.V. Krishnamurthy (2004a), Field evidence for geophysical detection of subsurface zones of enhanced microbial activity, Geophysical Research Letters, 31(23).

Atekwana, E.A., R.S. Rowe, D.D. Werkema, and F.D. Legall (2004b), The relationship of total dissolved solids measurements to bulk electrical conductivity in an aquifer contaminated with hydrocarbon, Journal of Applied Geophysics, 56(4), 281-294.

Baedecker, M.J., I.M. Cozzarelli, R.P. Eganhouse, D.I. Siegel, and P.C. Bennett (1993), Crude-oil in a shallow sand and gravel aquifer.3. Biogeochical reactions and mass-balance modeling in anoxic groundwater, Applied Geochemistry, 8(6), 569-586.

Bekins, B.A., I.M. Cozzarelli, E.M. Godsy, E. Warren, H.I. Essaid, and M.E. Tuccillo (2001), Progression of natural attenuation processes at a crude oil spill site: II. Controls on spatial distribution of microbial populations, Journal of Contaminant Hydrology, 53(3-4), 387-406.

Bennett, P.C., F.K. Hiebert, and W.J. Choi (1996), Microbial colonization and weathering of silicates in a petroleum-contaminated groundwater, Chemical Geology, 132(1-4), 45-53.

Börner, F., M. Gruhne, and J. Schön (1993), Contamination indications derived from electrical properties in the low frequency range, Geophysical Prospecting, 41(1), 83-98.

Cassidy, D.P., A.J. Hudak, D. Werkema, E.A. Atekwana, S. Rossbach, J.W. Duris, and W.A. Sauck (2002), In situ rhamnolipid production at an abandoned petroleum refinery, Soil & Sediment Contamination, 11(5), 769-787.

Cassidy, N.J. (2008a), Frequency-dependent attenuation and velocity characteristics of nano-to-micro scale, lossy, magnetite-rich materials, Near Surface Geophysics, 6(6), 341-355.

Cassidy, N.J. (2008b), GPR attenuation and scattering in a mature hydrocarbon spill: A Modeling study, Vadose Zone Journal, 7(1), 140-159.

Che-Alota, V., E.A. Atekwana, W.A. Sauck, and D.D. Werkema (2009), Temporal geophysical signatures from contaminant-mass remediation, Geophysics, 74(4), B113-B123.

Clement, T.P., B.S. Hooker, and R.S. Skeen (1996), Macroscopic models for predicting changes in saturated porous media properties caused by microbial growth, Ground Water, 34(5), 934-942.

Cozzarelli, I.M., B.A. Bekins, M.J. Baedecker, G.R. Aiken, R.P. Eganhouse, and M.E. Tuccillo (2001), Progression of natural attenuation processes at a crude-oil spill site: 1. Geochemical evolution of the plume, Journal of Contaminant Hydrology, 53(3-4), 369-385.

Cozzarelli, I.M., M.J. Baedecker, R.P. Eganhouse, and D.F. Goerlitz (1994), The geochemical evolution of low-molecular-weight organic-acids derived from the degradation of petroleum contaminants in groundwater, Geochimica Et Cosmochimica Acta, 58(2), 863-877.

Cozzarelli, I.M., Eganhouse, R., and Baedecker, M. (1990), Transformation of Monoaromatic hydrocarbons to organic acids in anoxic groundwater environment: Environmental Geology and Water Sciences, v. 16, no. 2, p. 135-141.

Davis, C. A., E. Atekwana, L. D. Slater, S. Rossbach, and M. R. Mormile (2006), Microbial growth and biofilm formation in geologic media is detected with complex conductivity measurements, Geophysical Research Letters, *33*(18).

Dekkers, M. J., H. F. Passier, and M. A. A. Schoonen (2000), Magnetic properties of hydrothermally synthesized greigite (Fe3S4)—II. High- and low-temperature characteristics, Geophysical Journal International, 141(3), 809-819.

Dobrin, M. B. (1960), Introduction to Geophysical Prospecting *Mc-Graw-Hill Book Co., Inc., New York*.

Eganhouse, R.P., M.J. Baedecker, I.M. Cozzarelli, G.R. Aiken, K.A. Thorn, and T.F. Dorsey (1993), Crude-oil in a shallow sand and gravel aquifer .2. Organic geochemistry, Applied Geochemistry, 8(6), 551-567.

Fredrickson J. K., J. M. Zachara, D. W. Kennedy, H. Dong, T. C. Onstott, N. W. Hinman, and S. M. Li (1998), Biogenic iron mineralization accompanying the dissimilatory reduction of hydrous ferric oxide by a groundwater bacterium. Geochimica et Cosmochimica Acta, 62,3239–3257.

Guo, H., and A. S. Barnard (2011), Proton transfer in the hydrogen-bonded chains of lepidocrocite: a computational study, Physical Chemistry Chemical Physics, 13(39), 17864-17869.

Guskos, N., et al. (2002), Photoacoustic, EPR and electrical conductivity investigations of three synthetic mineral pigments: hematite, goethite and magnetite, Materials Research Bulletin, 37(6), 1051-1061.

Hansel, C. M., Benner, S. G., and Fendorf, S., 2005, Competing Fe(II)-induced mineralization pathways of ferrihydrite: Environmental Science & Technology, v. 39, no. 18, p. 7147-7153.

Hansel, C. M., S. G. Benner, J. Neiss, A. Dohnalkova, R.K. Kukkadapu, and S.E. Fendorf (2003), Secondary mineralization pathways induced by dissimilatory iron reduction of ferrihydrite under advective flow. Geochimica et Cosmochimica Acta 67,16 2977-2992.

Kappler, A. and K.L. Straub (2005), geomicrobiological cycling of iron. In J.F. Banfield, J. Cervini-Silva, and K.H. Nealson, eds., Molecular geomicrobiology, 59, p. 85–108. Reviews in Mineralogy and geochemistry, Mineralogical Society of America, Chantilly, Virginia.

Karguppikar, A. M., and A. G. Vedeshwar (1988), Electrical and optical properties of natural iron pyrite (FeS2), physica status solidi (a), 109(2), 549-558.

Leroy P., A. Revil, A. Kemna, P. Cosenza, and A. Ghorbani (2008), Spectral induced polarization of water-saturated packs of glass beads, Journal of Colloid and Interface Science, 321 (1), 103-117.

Lesmes, D.P., and K.M. Frye (2001), Influence of pore fluid chemistry on the complex conductivity and induced polarization responses of Berea sandstone, Journal of Geophysical Research-Solid Earth, 106(B3), 4079-4090.

Lovley, D.R., M.J. Baedecker, D.J. Lonergan, I.M. Cozzarelli, E.J.P. Phillips, and D.I. Siegel (1989), Oxidation of aromatic contaminants coupled to microbial iron reduction. Nature; 339: 297–300.

Lovley, D.R., J.F. Stolz, G.L. Nord, and E.J.P. Phillips (1987), Anaerobic production of magnetite by a dissimilatory iron-reducing microorganism, Nature, 330(6145), 252-254.

Lovley, D.R., J.C. Woodward, and F.H. Chapelle (1994), Stimulated anoxic biodegradation of aromatic hydrocarbons using Fe(III) ligands. Nature; 370: 128–131.

Parkhomenko, E. I. (1982), Electrical resistivity of minerals and rocks at high temperature and pressure, Reviews of Geophysics, 20(2), 193-218.

Revil A., and N. Florsch, (2010), Determination of permeability from spectral induced polarization data in granular media, Geophysical Journal International, 181, 1480-1498, doi: 10.1111/j.1365-246X.2010.04573.x.

Revil, A., K. Koch, and K. Holliger (2012), Is it the grain size or the characteristic pore size that controls the induced polarization relaxation time of clean sands and sandstones?, Water Resour. Res., 48(5), W05602.

Revil, A., M. Schmutz, and M.L. Batzle (2011), Influence of oil wettability upon spectral induced polarization of oil-bearing sands, Geophysics, 76(5), A31-A36.

Rijal, M., Porsch, K., Appel, E., and Kappler, A., 2012, Magnetic signature of hydrocarbon-contaminated soils and sediments at the former oil field Hänigsen, Germany: Studia Geophysica Et Geodaetica, v. 56, no. 3, p. 889-908.

Rijal, M.L., E. Appel, E. Petrovsky, and U. Blaha (2010), Change of magnetic properties due to fluctuations of hydrocarbon contaminated groundwater in unconsolidated sediments, Environmental Pollution, 158(5), 1756-1762.

Simsa, Z., and V. A. M. Brabers (1988), Low temperature electric properties of magnetite Mn-ferrites, Magnetics, IEEE Transactions on, 24(2), 1910-1914.

Slater, L., D. Ntarlagiannis, Y.R. Personna, and S. Hubbard (2007), Pore-scale spectral induced polarization signatures associated with FeS biomineral transformations, Geophysical Research Letters, 34(21).

Thullner, M., J. Zeyer, and W. Kinzelbach (2002), Influence of microbial growth on hydraulic properties of pore networks, Transport in Porous Media, 49(1), 99-122.

Vinegar, H.J., and M.H. Waxman (1984), Induced polarization of shaly sands, Geophysics, 49(8), 1267-1287.

Waxman, M.H., and L.J.M. Smits (1968), Electrical conductivities in oil-bearing shaly sands, Society of Petroleum Engineers Journal, 8(2), 107-&.

Weber, K.A., M.M. Urrutia, P.F. Churchill, R.K. Kukkadapu, and, E.E. Roden (2006), Anaerobic redox cycling of iron by freshwater sediment microorganisms. Environmental Microbiology, 8, 100–113.

Werkema, D.D., E.A. Atekwana, A.L. Endres, W.A. Sauck, and D.P. Cassidy (2003), Investigating the geoelectrical response of hydrocarbon contamination undergoing biodegradation, Geophysical Research Letters, 30(12).

Whitman, W. B., Coleman, D. C., and Wiebe, W. J., 1998, Prokaryotes: The unseen majority: Proceedings of the National Academy of Sciences of the United States of America, v. 95, no. 12, p. 6578-6583.

Williams, K.H., D. Ntarlagiannis, L.D. Slater, A. Dohnalkova, S.S. Hubbard, and J.F. Banfield (2005), Geophysical imaging of stimulated microbial biomineralization, Environmental Science & Technology, 39(19), 7592-7600.

Zachara J. M., R. K. Kukkadapu, J. K. Fredrickson, Y. A. Gorby, and S. C. Smith (2002), Biomineralization of poorly crystalline Fe(III) oxides by dissimilatory metal reducing bacteria (DMRB). Geomicrobiology Journal 19, 179–207.

Zywietz, F., and R. Knochel (1986), Dielectric-properties of co-gamma-irradiated and microwave-heated rat-tumor and skin measured invivo between 0.2 and 2.4 ghz, Physics in Medicine and Biology, 31(9), 1021-1029.

PAPER 1

MAGNETIC SUSCEPTIBILITY AS A PROXY FOR INVESTIGATING MICROBIALLY MEDIATED IRON REDUCTION

2.0. ABSTRACT

We investigated magnetic susceptibility (MS) variations in hydrocarbon contaminated sediments. Our objective was to determine if MS can be used as an intrinsic bioremediation indicator due to the activity of iron-reducing bacteria. A contaminated and an uncontaminated core were retrieved from a site contaminated with crude oil near Bemidji, Minnesota and subsampled for MS measurements. The contaminated core revealed enriched MS zones within the hydrocarbon smear zone, which is related to iron-reduction coupled to oxidation of hydrocarbon compounds and the vadose zone, which is coincident with a zone of methane depletion suggesting aerobic or anaerobic oxidation of methane is coupled to iron-reduction. The latter has significant implications for methane cycling. We hypothesize that MS can serve as a proxy for intrinsic bioremediation by iron-reducing bacteria and for the application of geophysics to iron cycling studies.

2.1. INTRODUCTION

The Deepwater Horizon spill in the Gulf of Mexico is a reminder of the environmental threat of hydrocarbon contamination and the need for technological advancements for detecting, monitoring, and remediating hydrocarbon contamination. Due to the relationship between magnetic minerals and redox reactions associated with hydrocarbon seeps, magnetic susceptibility (MS) has been used as a possible tool for oil exploration (e.g., Saunders et al., 1999). In surficial sediments, MS traditionally is used for climate studies (e.g., Kukla et al., 1988), mapping heavy metal soil contamination (e.g., Hanesch and Scholger, 2002), and identifying sediment sources and transport trends (Ellwood et al., 2006). MS has recently emerged as a tool for investigating iron cycling mediated by microbial activity (e.g., Porsch et al., 2010; Rijal et al., 2010).

This work investigates MS variations in a hydrocarbon contaminated aquifer where methanogenesis and iron-reduction are the main terminal electron accepting processes (Baedecker et al., 1993). Our objective was to determine if MS could be an indicator of the presence of intrinsic hydrocarbon degradation by iron-reducing bacteria. Our results suggest enhancements in MS are due to the precipitation of magnetite coupled to iron-reduction as related to; (1) anaerobic oxidation of hydrocarbon compounds within the smear zone and (2) aerobic or anaerobic oxidation of methane within the vadose zone, which provides additional field evidence linking anaerobic oxidation of methane to iron-reduction and suggests significant implications for methane cycling in terrestrial environments.

2.2. SITE HISTORY

The crude oil spill near Bemidji, Minnesota (Figure 1), is a field laboratory for investigating biogeophysical signatures associated with the intrinsic bioremediation. In August 1979, a high pressure crude oil pipeline ruptured, releasing 1,700,000 L of crude oil. The study site consists of ~ 20 m-thick of moderately calcareous sand and outwash glacial deposits overlying clayey till of unknown thickness (Bennett et al., 1993). Iron minerals in sediments include goethite, hematite, magnetite, ferrihydrite, and maghemite (Bekins et al., 2001).

The uncontaminated groundwater is aerobic with dissolved oxygen concentrations between 8 and 9 mg/L, dissolved organic carbon of 2.8 mg/L as C, and low levels of nitrate generally <0.2 mg/L, and sulfate at 2.9 mg/L (Bennett et al., 1993). The aquifer is divided in the vicinity of the oil body into anoxic, transition, and background zones. In the anoxic portion, hydrocarbons are oxidized predominantly by iron reduction (Lovley et al., 1989) and methanogenesis (e.g., Baedecker et al., 1993). Bekins et al. (2001) show two zones of methanogenic activity with CH_4 concentrations greater than 15 mg/L. The vadose zone vapor plume near the oil body has low O_2 (< 2%) and high CO_2 (>10%) and CH_4 (>15%) levels.

2.3. MATERIALS AND METHODS

2.3.1 Retrieval of Cores

Two ~5-cm diameter cores were retrieved from contaminated (C1010) and uncontaminated (C1006) locations (Figure 1). Whereas the contaminated core was continuously collected, two segments of core were collected from the uncontaminated location. The cores were collected by advancing a core barrel with a polycarbonate liner

ahead of a hollow-stem auger. The cores within the smear zone or below the water table were collected with a freezing drive shoe (Murphy and Herkelrath, 1996), preserved in coolers unexposed to the atmosphere, and shipped to the laboratory at Oklahoma State University by an overnight courier.

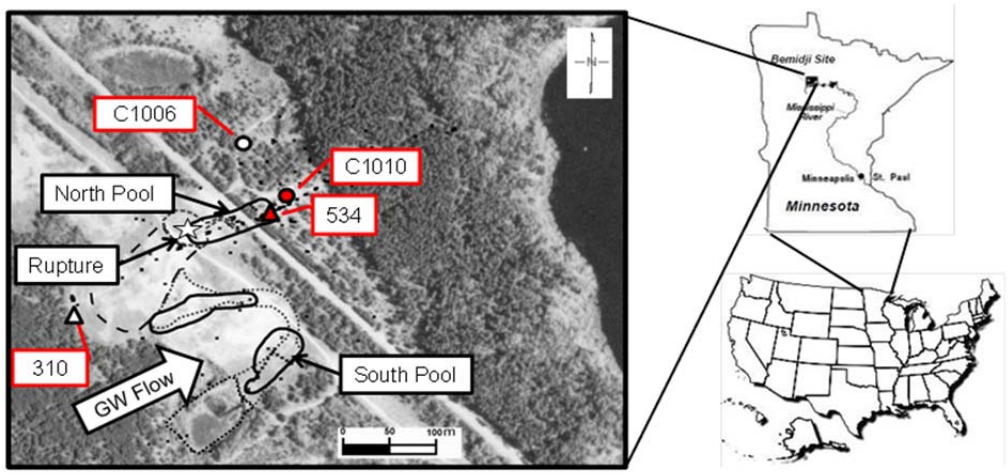

Figure 1. Study area showing the location of core samples (circles) and gas data (triangles) at contaminated (closed symbols) and uncontaminated (opened symbols) boreholes. 310 and 534 are vadose zone gas sampling boreholes.

2.3.2 MS Measurements and Iron Analysis

Sub-samples of ~10 grams were taken at 5 to 15 cm intervals along the cores. Sub-samples were oven dried at 50°C for 24 hours then analyzed for MS using a Bartington MS2 magnetic susceptibility meter (1.2566 x 10^{-11} m^3/kg sensitivity). Then the same samples were used to quantify iron content. The mass of magnetic particles retained by a bar magnet was measured and the percentage of the iron-rich material per sample was determined.

2.3.3 Gas data

Vapor wells 534 (contaminated) and 310 (uncontaminated) (Fig. 1) consisted of permanently installed vapor probes generally spaced at 50- to 100-cm depth intervals in the unsaturated zone, from 1 m below land surface to 1 m above the water table (Chaplin et al., 2002). Each probe was constructed of 0.16- to 0.64-cm outside diameter stainless steel tubing with 5 to 10-cm long screens at the bottom. The probes were installed in 10-cm-diameter augered holes, which were backfilled with native sand, and included a bentonite seal between each screened interval. The gas samples were obtained in gas-tight glass syringes using a peristaltic pump and analyzed on-site using a SRI® 8610C Gas Chromatograph (GC). The GC was configured using a 1.0-mL fixed-loop injection and an internal air compressor. Fixed gas (Ar, O_2, CO_2, and CH_4) analyses were determined with a thermal conductivity detector (TCD) and a SRI® CTR-1 double-packed column. Concentrations of gases were quantified in weight percent using gas standards containing mixtures of Ar, O_2, CO_2, and CH_4.

2.4. RESULTS

2.4.1.Magnetic Susceptibility

The contaminated core showed two zones of high MS (Figure 2a) versus the uncontaminated core (Figure 3a). The first zone was located from ~423 m at the base of the free hydrocarbon to 426 m at the top of the groundwater table (GWT) where the MS values ranged from 75 to 299 $x10^{-8}$ m^3kg^{-1} reaching a maximum at 423.5 m (Figure 2c). The second zone was between 428-429 m where the MS values ranged between 88 to $218x10^{-8}$ m^3kg^{-1} to a maximum at ~429 m (Figure 2a). Another zone of high MS was observed at 427.2 m. This high MS zone occurs within the vadose zone with no

corresponding free or residual hydrocarbon contamination (Figure 2c). The MS of the uncontaminated core showed relatively small variations with no anomalous zones and values ranging from 40 to 145x10^{-8} $m^3.kg^{-1}$ (Figure 3a).

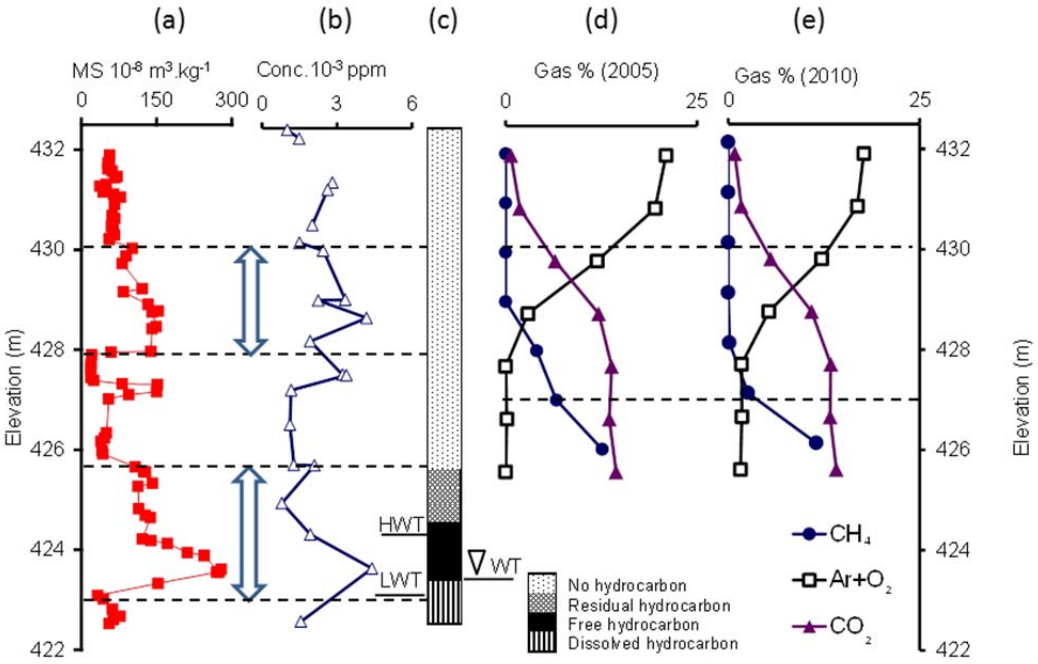

Figure 2. (a) Magnetic susceptibility, (b) iron wt %, (c) hydrocarbon distribution within core, gas concentrations in (d) 2005, and (e) 2010 along the contaminated core (C 1010). HWT: Highest water level, LWT: Lowest water level and WT: Water Table during the time of measurements. Elevation above mean sea level (amsl). The gas data are from location 534 located 10 m from C1010.

2.4.2. Magnetic minerals analysis

The measurements of the iron wt % in the uncontaminated core showed no anomalous concentrations with values ranging from 0.07 to 0.22 and an average value of 0.14 wt %. In contrast, the contaminated core showed elevated values between 0.19 to

0.44 wt %, reaching a maximum at 423.5 m at depths coincident with higher MS (Figure 2b). In the 428-430 m elevation interval, the iron wt % ranged between 0.19 to 0.42 wt % with a maximum at 429 m. The correlation between MS and magnetite, obtained by plotting MS versus magnetite suggests that magnetite is responsible for the MS variations with an R^2 of 0.817 and 0.967 for the contaminated and uncontaminated cores, respectively. XRD analyses (Supplemental Figure) suggested that magnetite was the dominant phase.

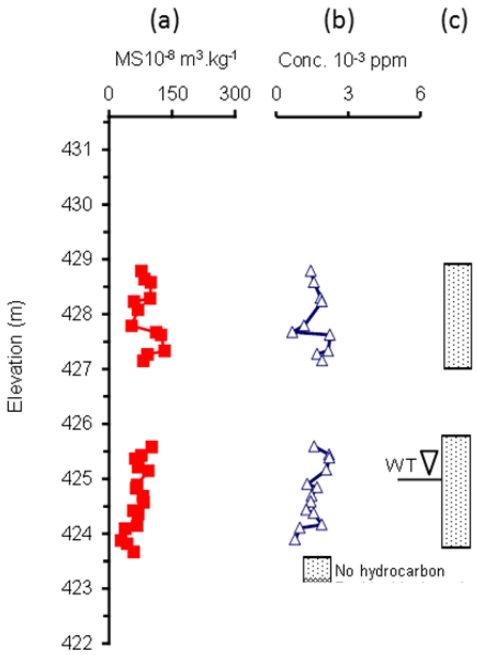

Figure 3. (a) Magnetic susceptibility, (b) iron wt %, and (c) hydrocarbon distribution in two 2-m zones along the uncontaminated borehole (C 1006). WT: Water Table during the time of measurements. Elevation above mean sea level (amsl).

2.4.3. Distribution of Ar + O_2, CH_4 and CO_2

In 2005, the CO_2 concentrations increased from nearly 0.7% at ground surface to 6.5% at 430 m and 12.2% at 429 m. Ar and O_2 concentrations decreased downward to less than 11.9% at 430 m to 2.9% at 429 m and are depleted at 428 m. CH_4 showed

depletion upwards from about 4% at 427m to 0% at 429 m (Figure 2d). These data define a transition zone from ~427 m to 430 m where O_2 and CH_4 are depleted and CO_2 is enriched. The same trends occur in the 2010 data; however, the transition zone has shifted to a lower elevation (Figure 2e). The uncontaminated gas concentration profile showed no variability as compared to atmospheric values.

2.5. DISCUSSION AND CONCLUSIONS

Geochemical and microbial studies suggest iron reduction is an important terminal electron acceptor process occurring within the anaerobic plume (e.g. Baedecker et al., 1993). In addition, iron-reducing bacteria such as *Geobacter bemidjiensis* sp. and *Geobacter psychrophilus* sp occur in the contaminated aquifer (Nevin et al., 2005). During iron reduction, Fe^{3+} is converted to Fe^{2+} which can be oxidized by the protons of water to form magnetite:

$$3\ Fe(OH)_2 \rightarrow Fe_3O_4\downarrow + H_2 + 2\ H_2O \quad \ldots\ldots(1).$$

2.5.1. Smear Zone

The smear zone above the GWT (423.5-425 m) shows the highest MS values and iron wt % (Figure 2a-c). Biogeophysical investigations at other hydrocarbon contaminated sites have documented the highest value of bulk electrical conductivity within this smear zone and suggested it to be most biologically active (Werkema et al., 2003). Additionally, MS studies by Rijal et al. (2010) show concentrations of magnetic parameters increasing towards the top of the GWT. Thus, we infer this enriched zone of magnetite is due to the anaerobic oxidation of hydrocarbons by iron-reducing bacteria (Lovley et al., 1989). Microbial data showed culturable iron reducers were present in the oil layer in 1997 (Bekins et al., 1999).

2.5.2. Unsaturated zone

The zone of enriched magnetite occurring in the vadose zone (427-430 m) (Figure 2a) can be explained by: (1) naturally occurring higher concentration of magnetite within the sediments in this zone, (2) precipitation of magnetite (eq. 1 and 2) related to past hydrocarbon vapors in the vadose zone, (3) precipitation of magnetite (eq. 1), related to aerobic oxidation of methane (eq. 2) which releases water protons that can oxidize Fe $(OH)_2$ to magnetite,

$CH_4 + 2O_2 \rightarrow CO_2 + 2H_2O$…….....…….……(2).

or (4) the precipitation of magnetite resulting from anaerobic oxidation of methane (AOM) coupled to iron reduction.

Although there are presently no hydrocarbon vapors present in the vadose zone, vapors were present in the past (Chaplin et al. 2002). Hence, the zone of enriched magnetite occurring in the vadose zone at the 427-430 m elevation (Figure 2a) could represent a relict process of bacterial oxidation of the hydrocarbon vapors coupled to iron reduction. Nevertheless, we favor hypotheses 3 and 4 for the following reason. The gas data (Figures 2d-e) suggest a transition in the methane and oxygen plots crossing at 428.3 m (2005) and 427.2 m (2010), where the total depletion of methane occurs. Also, culturable methanotroph microbial population numbers peak within this zone (Molins et al., 2010; data not shown). This has led some to suggest the aerobic oxidation of methane within this zone (Amos et al., 2005). It is possible that the precipitation of magnetite in this zone could be linked to the aerobic oxidation of methane (eq. 1 and 2).

The precipitation of magnetite resulting from the anaerobic oxidation of methane (AOM) coupled to iron reduction is also possible. Whereas AOM coupled to sulfate reduction is documented in marine environments (e.g., Hoehler et al., 1994), AOM

coupled to metal reduction is not common and has yet to be definitively demonstrated. There are also no known microorganisms capable of this process (Beal et al., 2009). Nonetheless, recent studies postulate that AOM coupled to metal reduction is likely to occur (e.g., Beal et al., 2009; Crowe et al., 2011). Beal et al. (2009) show AOM in the absence of sulfate if birnessite or ferrihydrite is present. Crowe et al., (2011) document that, despite high abundances of Fe (hydr)oxides in lake sediments, more than 50% of authigenic organic matter was degraded through methanogenesis, suggesting methane oxidation and Fe(III) reduction coupling. This mechanism is as follows:

(1) AOM coupled with ferrihydrite (simplified as $Fe(OH)_3$) reduction (Beal et al., 2009).

$CH_4+8Fe(OH)_3+ 15H^+ \rightarrow HCO_3^- +8Fe^{2+}+ 21H_2O$ ……..(3).

Part of the Fe^{2+} reacts with the small amounts of O_2 present, thereby precipitating magnetite:

$3\ Fe(OH)_2 + ½\ O_2 \rightarrow Fe(OH)_2.2\ FeOOH + H_2O$ ……..……(4).

$Fe(OH)_2.2\ FeOOH \rightarrow Fe_3O_4\downarrow + 2H_2O$ …..……..…….(5).

The remaining $Fe(OH)_2$ can be oxidized by water protons to form magnetite (eq. 1).

Geochemical studies at this site show low levels of nitrate (44.8 μg/L as N_2) and sulfate (2.9 mg/L) (Bennett et al., 1993), which, in addition to elevated precipitation of magnetite, supports our argument that this is a zone of methane oxidation coupled with iron reduction. Our study suggests that MS measurements may aid in field investigations of this process. AOM coupled to iron reduction has significant implications for methane cycling in terrestrial environments. Biogeophysical studies can help guide microbial sampling thereby advancing microbial ecology studies of new microbial species associated with bioremediation.

2.6. REFERENCES

Amos, R.T., Mayer, K.U., Bekins, B.A., Delin, G.N., Williams, R.L. (2005), Use of dissolved and vapor-phase gases to investigate methanogenic degradation of petroleum hydrocarbon contamination in the subsurface, *Water Resources Research*, 41(2), W02001

Baedecker, M. J., I. M. Cozzarelli, R. P. Eganhouse, D. I. Siegel, and P. C. Bennett (1993), Crude-oil in a shallow sand gravel aquifer 3. Biogeochemical reactions and mass-balance modelling in anoxic groundwater, *Applied Geochemistry*, *8*(6), 569-586.

Beal, E. J., C. H. House, and V. J. Orphan (2009), Manganese- and Iron-Dependent Marine Methane Oxidation, *Science*, *325*(5937), 184-187.

Bekins, B.A., Godsy, E.M., Warren, E., (1999). Distribution of microbial physiologic types in an aquifer contaminated by crude oil, *Microbial Ecology* 37, 263–275.

Bekins, B. A., I. M. Cozzarelli, E. M. Godsy, E. Warren, H. I. Essaid, and M. E. Tuccillo (2001), Progression of natural attenuation processes at a crude oil spill site: II. Controls on spatial distribution of microbial populations, *Journal of Contaminant Hydrology*, *53*(3-4), 387-406.

Bennett, P. C., D. E. Siegel, M. J. Baedecker, and M. F. Hult (1993), Crude oil in a shallow sand and gravel aquifer—I. Hydrogeology and inorganic geochemistry, *Applied Geochemistry*, *8*(6), 529-549.

Chaplin, B. P., G. N. Delin, R. J. Baker, and M. A. Lahvis (2002), Long-term evolution of biodegradation and volatilization rates in a crude oil-contaminated aquifer, *Bioremediation Journal*, *6*, 237-255.

Crowe, S. A., Katsev, S., Leslie, K., Sturm, A., Magen, C., Nomosatryo, S., Pack, M. A., Kessler, J. D., Reeburgh, W. S., Roberts, J. A., GonzA´ Lez, L., Douglas Haffner, G., Mucci, A., Sundby, B., and Fowle, D. A. (2011), The methane cycle in ferruginous Lake Matano, Geobiology, 9(1), 61-78.

Ellwood, B. B., W. L. Balsam, and H. H. Roberts (2006), Gulf of Mexico sediment sources and sediment transport trends from magnetic susceptibility measurements of surface samples, *Marine Geology*, *230*(3-4), 237-248.

Hanesch, M., and Scholger, R., (2002), Mapping of heavy metal loadings in soils by means of magnetic susceptibility measurements, *Environmental Geology*, *42*(8), 857-870.

Hoehler, T. M., M. J. Alperin, D. B. Albert, and C. S. Martens (1994), Field and laboratory studies of methane oxidation in an anoxic marine sediment: Evidence for a methanogen-sulfate reducer consortium, *Global Biogeochemical Cycles*, 8(4), 451-463.

Kukla, G., F. Heller, L. X. Ming, X. T. Chun, L. T. Sheng, and A. Z. Sheng (1988), Pleistocene climates in China dated by magnetic susceptibility, *Geology*, *16*(9), 811-814.

Lovley, D. R., M. J. Baedecker, D. J. Lonergan, I. M. Cozzarelli, E. J. P. Phillips, and D. I. Siegel (1989), Oxidation of aromatic contaminants coupled to microbial iron reduction, *Nature*, *339*(6222), 297-300.

Molins, S., K.U. Mayer, R.T. Amos, and B.A. Bekins (2010), Vadose zone attenuation of volatile organic compounds at a crude oil spill site – Interactions between

multicomponent gas transport and biogeochemical reactions, *Journal of Contaminant Hydrology*, 112, 15-29.

Murphy, F., Herkelrath, W.N., (1996), A sample-freezing drive shoe for a wire line piston core sampler, *Ground Water Monitoring and Remediation* 16, 86-90.

Nevin, K. P., D. E. Holmes, T. L. Woodard, E. S. Hinlein, D. W. Ostendorf, and D. R. Lovley (2005), Geobacter bemidjiensis sp. nov. and Geobacter psychrophilus sp. nov., two novel Fe(III)-reducing subsurface isolates, *International Journal of Systematic and Evolutionary Microbiology*, *55*(4), 1667-1674.

Porsch, K., U. Dippon, M. L. Rijal, E. Appel, and A. Kappler (2010), In-situ magnetic susceptibility measurements as a tool to follow geomicrobiological transformation of Fe minerals, *Environmental Science & Technology*, *44*(10), 3846-3852.

Rijal, M. L., E. Appel, E. Petrovský, and U. Blaha (2010), Change of magnetic properties due to fluctuations of hydrocarbon contaminated groundwater in unconsolidated sediments, *Environmental Pollution*, *158*(5), 1756-1762.

Saunders, D. F., K. R. Burson, and C. K. Thompson (1999), Model for hydrocarbon microseepage and related near-surface alterations, *American Association of Petroleum Geologists Bulletin*, *83*(1), 170-185.

Werkema, D. D., Jr., E. A. Atekwana, A. L. Endres, W. A. Sauck, and D. P. Cassidy (2003), Investigating the geoelectrical response of hydrocarbon contamination undergoing biodegradation, *Geophys. Res. Lett.*, *30*(12), 1647.

PAPER 2

EVIDENCE THAT BIOMETALLIC MINERAL PRECIPITATION ENHANCES THE COMPLEX CONDUCTIVITY RESPONSE AT A HYDROCARBON CONTAMINATED SITE

3.0. ABSTRACT

The complex conductivity signatures of a hydrocarbon contaminated site, undergoing biodegradation, near Bemidji, Minnesota were investigated. This site is characterized by a biogeochemical process where iron reduction is coupled with the oxidation of hydrocarbon contaminants. The biogeochemical transformations have resulted in biometallic mineral precipitates of different iron mineral phases such as magnetite, ferroan calcite, and siderite. Our main objective was to elucidate the major factors controlling the complex conductivity response at the site. The site has two main oil pools; a North and South pool. We acquired laboratory complex conductivity measurements along four cores retrieved from the North Pool. We find that the real (σ') and imaginary (σ'') conductivity are not always higher for samples from within the oil plume compared to background uncontaminated samples. Controlled experiments indicate that variations in electrolytic conductivity and water content are unlikely to account for the higher σ'' observed within the smear zone. Instead, using magnetite as an example of the bio-metallic minerals in the smear zone at the site,

a clear increase in the σ″ response with increasing magnetite content was observed. The presence of bio-metallic mineral phases (like magnetite) as well as electroactive dissolved iron(II) within the smear zone may explain the increase in σ″ observed for the contaminated cores. Thus, we postulate that, the presence of bio-metallic mineral phases impacts complex conductivity signatures and should be considered in the interpretation of complex conductivity data from oil contaminated sites undergoing intrinsic bioremediation.

3.1. INTRODUCTION

Previous studies have suggested the use of geophysical methods as complementary, rapid, cost-effective and minimally-invasive tools for detecting and monitoring the extent and fate of oil spills in the subsurface (Werkema et al., 2003; Atekwana et al., 2004a; Che-Alota et al., 2009, Atekwana and Atekwana 2010). Among the different geophysical tools, complex conductivity has been suggested as a technique with high sensitivity to the presence of contaminants (Olhoeft, 1985; Börner et al., 1993; Vanhala et al., 1992; Revil et al., 2011, Schmutz et al., 2010, 2012) as well as accompanying bio-physicochemical processes associated with hydrocarbon biodegradation (Abdel Aal et al., 2004; 2006). Moreover, the complex conductivity has been successfully applied at the field scale for imaging hydrocarbon contamination (Kemna et al., 2004; Flores Orozco et al., 2012). Nonetheless, the interpretation of complex conductivity data from field sites undergoing active microbial degradation remains challenging partly because several factors may contribute to the observed complex conductivity response.

The presence of oil stimulates biological activity, resulting in bio-physicochemical changes induced in the subsurface during the biodegradation of hydrocarbons by

microbes (Cozzarelli et al., 1994; Cozzarelli et al., 2001; Cassidy et al., 2002). Microbes provided with an organic carbon source and nutrients can result in (1) an increase in cell density and the formation of biofilms on the grain surfaces and between pore openings in rocks and sediments that induce physical changes in the porous material itself (Clement et al., 1996; Thullner et al., 2002; Atekwana and Slater, 2009; Abdel Aal et al., 2010, Atekwana and Atekwana, 2010) and (2) the production of organic and carbonic acids that enhance the weathering of aquifer solids causing an increase in the surface roughness of the mineral grains and the ionic strength of the pore water (Atekwana et al., 2004b; Abdel Aal et al., 2006).

The presence of terminal electron acceptors (TEA's) governs nutrient utilization by microbes during the breakdown of organic carbon (Bekins et al., 2001; Cozzarelli et al., 2001). TEA's are sequentially utilized from O_2, NO_3^-, Fe(III), Mn (IV), SO_4^{2-}, and CO_2. Some iron(III)-reducing microorganisms can use hydrocarbons as a carbon source to reduce iron(III) to Fe(II) (Lovley et al., 1989). When hydrocarbon biodegradation is coupled to iron reduction it can lead to the formation of ferrous bio-minerals such as magnetite (Lovley et al., 1987; Rijal et al., 2010), pyrite (Prommer et al., 1999), ferroan calcite (Baedecker et al., 1992) and siderite (Tuccillo et al., 1999). For example, magnetite can be formed through either biologically induced (abiotic) mineralization or biologically controlled (biotic) mineralization. In the biologically induced mineralization magnetite can be nucleated and grow abiotically by chemical reactions involving byproducts as a result of biotic metabolic activity, while during biologically controlled mineralization, magnetite can be synthesized at a specific location within or on the cell (Bazylinski and Frankel, 2003). In these two pathways, iron(III) can be converted to

iron(II), then magnetite can be precipitated either by nucleation or growth that is controlled by ferrous iron concentration and/or pH (Hansel et al., 2005).

In several recent studies, magnetic susceptibility data from hydrocarbon contaminated sites have documented zones of enhanced magnetic susceptibility within the smear zone coincident with the free phase hydrocarbon plume (Rijal et al., 2010; 2012; Mewafy et al., 2011). In these studies, magnetite was documented as the dominant mineral within the enhanced zone of magnetic susceptibility, suggesting biomineralization due to iron reduction. We test the effect of bio-metallic mineral phases such as magnetite should significantly impact the complex conductivity response at hydrocarbon contaminated sites.

In this study, we acquired laboratory complex conductivity measurements from a hydrocarbon contaminated site where hydrocarbon biodegradation has been extensively documented. Additionally, we conducted several controlled experiments simulating the field conditions to aid interpretation of our results. Our specific objective was to elucidate the major factors controlling the complex conductivity response at hydrocarbon contaminated sites undergoing biodegradation.

3.2. SITE HISTORY

The National Crude Oil Spill Fate and Natural Attenuation Research Site at Bemidji, MN (Figure 1) is a natural laboratory available for investigating bio-physicochemical processes associated with the intrinsic bioremediation of a crude oil spill (Eganhouse et al., 1993; Cozzarelli et al., 2001). In August 1979, a high pressure crude oil pipeline ruptured, releasing 1,700,000 L of crude oil. Oil pooled in low-lying areas (~2000 m^2) over a total area of 6,500 m^2 to the southwest of the pipeline, forming the South and

North Pools (Figure 1). According to Essaid et al. (2011), the oil saturation of the soil was ~0.62 near the center of the South Pool which decreased to less than 0.20 within a large area around the pool. For the North Pool a maximum oil saturation of 0.74 was measured in the down gradient part of the oil body with a smear zone extending more than 2 m around the water table with ~ 1 m seasonal fluctuation. The water table is about 2.7 m below the land surface at the South oil Pool and about 8 m below land surface at the North oil Pool (Delin et al., 1999).

The site geology consists of pitted sand and gravel outwash and moderately calcareous silty sand (about 20 m thick) and outwash glacial deposits overlying clayey till of unknown thickness (Bennett et al., 1993). The north plume has been the focus of intensive geochemical (Cozzarelli et al., 2010) and microbiological studies (Bekins et al., 2001). Studies on the South Pool revealed that the oil body was more than 70 m long and asymmetric, with more oil present downgradient with highest oil saturation (~0.62) near the center of the oil body (Dillard et al., 1997). The uncontaminated groundwater is aerobic with dissolved oxygen concentrations between 8 and 9 mg/L, dissolved organic carbon of 2.8 mg/L as C, and low levels of nitrate at 44.8 µg/L as N_2 and sulfate at 2.9 mg/L (Bennett et al., 1993).

Geochemical and microbial studies suggest iron reduction is an important terminal electron acceptor process occurring within the anaerobic plume (e.g., Baedecker et al., 1993). In addition, iron-reducing bacteria such as *Geobacter bemidjiensis* sp. and *Geobacter psychrophilus* sp occur in the contaminated aquifer (Nevin et al., 2005). Tuccillo et al. (1999) observed reduced levels of iron(III) in the sediments closest to and underneath the oil body, whereas iron(II) values under the oil body (19.2 µmol/g) are as

much as 4 times those in the background sediments (4.6 μmol/g). They demonstrated that magnetite was abundant in the ferromagnetic fraction of the bulk sediment, representing roughly 0.5% of the bulk sediment in addition to siderite and ferroan calcite. A recent study by Mewafy et al. (2011) documented an enhanced zone of magnetic susceptibility within the smear zone and in the vadose zone of the contaminated location and suggested that this enhancement in magnetic susceptibility is due to an increase in magnetite content resulting from the coupling of hydrocarbon oxidation with iron reduction.

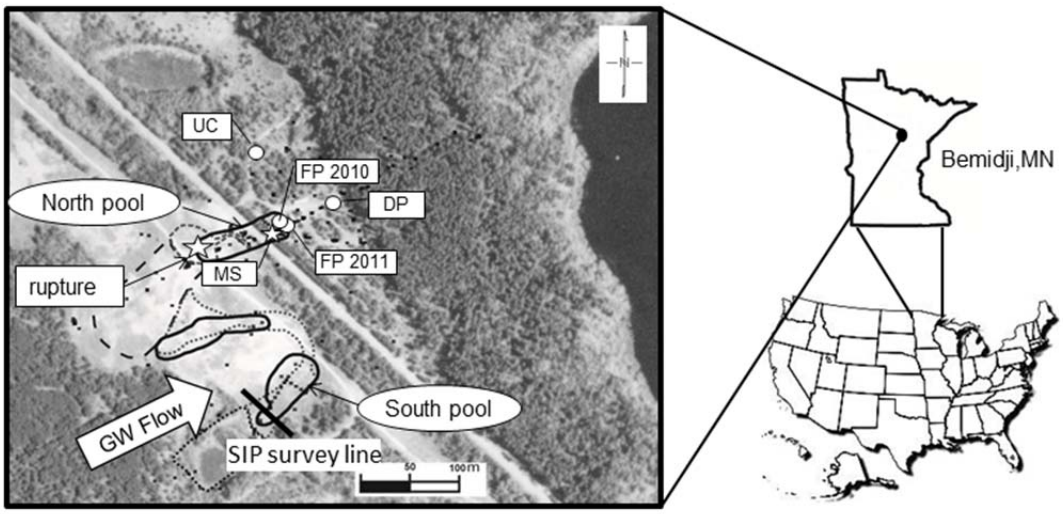

Figure 1. Plan view of the Bemidji oil spill site showing locations of the cores retrieved from the free phase plume (FP), dissolved plume (DP) and uncontaminated (UC), and the field complex conductivity survey line crossing the South Pool. MS: Bore hole magnetic susceptibility location.

3.4. COMPLEX CONDUCTIVITY

Silver-chloride non-polarizable electrodes were used to measure the resulting difference of the electrical potential across a sample in response to current flow. The impedance magnitude ($|\sigma|$) and phase (φ) of the sample were recorded relative to a

precision reference resistor upon stimulus with a sine-wave current. The measured frequency dependent complex conductivity σ* (ω) behavior of a porous medium can be generally represented with an in-phase (real) conductivity component (σ′) or electromigration term, and a quadrature (imaginary) conductivity component (σ″) or polarization term. The imaginary conductivity exhibits polarization (in our frequency range) that is a reversible storage of electrical charges occurring at interfaces. Both the real and imaginary conductivities can be calculated as follows:

$$\sigma' = |\sigma| \cos \varphi \tag{1}$$

$$\sigma'' = |\sigma| \sin \varphi \tag{2}$$

The real conductivity of the porous material σ' can be written as a function of the formation factor F, the pore water conductivity σ_w and saturation S_w by,

$$\sigma' = (1/F) S_w^{\,n} \sigma_w + \sigma'_{\text{int}}, \tag{3}$$

where n denotes the second Archie exponent (Archie, 1942), $F = \phi^{-m}$ (Archie, 1942) denotes the formation factor with m being the cementation exponent, S_w is the water saturation, ϕ the porosity, and σ'_{int} denotes an interfacial conductivity term. A common assumption is that the electrolytic conductivity σ_w and interfacial conductivity σ'_{int} add in parallel (Waxman and Smits, 1968; Vinegar and Waxman, 1984). This assumption of parallel conduction paths may not always be realistic, especially at low pore water conductivities (Revil, 2012a). The interfacial conductivity (σ'_{int}) is controlled by surface area, surface charge density, and surface ionic mobility at the grain-fluid interface (Lesmes and Frye, 2001; Lesmes and Morgan, 2001; Revil and Glover, 1998).

The imaginary conductivity can be related to a variety of polarization mechanisms including the membrane polarization (Marshall and Madden, 1959), the polarization of the inner part of the electrical double layer coating the surface of the grains (the Stern layer, e.g., Lesmes and Frye, 2001; Revil and Florsch, 2010) and electrode polarization (Wong, 1979). In the absence of metallic minerals, two main mechanisms cause the polarization in the low frequency range (<100Hz); electrochemical polarization (Leroy et al., 2008) and the Maxwell-Wagner polarization at frequency (>10Hz); (Revil and Florsch, 2010).

The presence of metallic conductors contributes a polarization enhancement, electrode polarization, which results from the tendency for electron transport through the metal (Marshall and Madden, 1959; Pelton et al., 1978; Wong, 1979). The application of an external current results in electrochemical redox reactions and electromigration of redox ionic species such as iron(II)/iron(III) as active ions that results in a potential difference to be established between the electrode and the solution. Passage of current disturbs the equilibrium causing charge pile up at the electrode-electrolyte interface. On current termination, the original equilibrium (in which a thin layer of negative ions is fixed to the metal electrode) is gradually re-established as the extra piled-up charge diffuses back into the electrolyte.

3.5. MATERIALS AND METHODS

3.5.1. Retrieval of Cores

A total of four ~5-cm diameter cores were retrieved from the site. Two cores were collected in July 2010, one from the free phase plume, and one from the uncontaminated location. Two additional cores were retrieved in July 2011, one from the free phase

plume and one from the dissolved phase plume (Figure 1). All the cores extended from the ground surface to below the water table except for the uncontaminated core where two segments of core were collected, representing the vadose and saturated zones. All four cores were retrieved using a hollow-stem auger by advancing a core barrel with a polycarbonate liner. The cores within the smear zone, or below the water table, were collected with a freeze drive shoe (Prommer et al., 1999), preserved in coolers unexposed to the atmosphere, and shipped to the laboratory at Rutgers-Newark University for measurements that started 10 days later.

3.5.2. Laboratory complex conductivity Measurements for North Pool Cores

Complex conductivity measurements were made on core segments ~ 35 cm long (Figure 2) with 5 cm spacing between the potential electrodes. We saturated 2010 cores with NaCl solution with the (0.085S/m) and (0.025S/m) for the cores retrieved from the contaminated and uncontaminated locations respectively to have a good contact; however we were able to acquire the measurements for 2011 cores without saturation. The current electrodes (Ag) and the potential electrodes (Ag-AgCl) were connected to a National Instruments four-electrode dynamic signal analyzer (Slater and Lesmes, 2002). The phase lag between the current stimulus-voltage signal and the impedance magnitude was measured at 30 frequencies, spaced at equal logarithmic intervals between 0.001 and 1000 Hz. Current was injected at spiral electrodes located at sample ends while the sample voltage was measured using point potential electrodes located just outside the current flow path. A preamplifier boosted the input impedance on the voltage channel and prevented current leakage into the circuitry.

3.5.3. Control Experiments

3.5.3.1 Complex conductivity signatures associated with saturation and fluid conductivity

Since the complex conductivity varies strongly as a function of fluid chemistry (Lesmes and Frye, 2001) and water saturation (Ulrich and Slater, 2004; Revil et al., 2012b, Breede et al., 2012), we conducted control experiments to constrain the variability in the complex conductivity (i.e., real and imaginary parts) of our samples that could be independent of the effects of contamination and associated microbial degradation. We conducted these experiments over a narrower frequency range (1-1000 Hz)..

To test the effect of moisture content, we acquired complex conductivity measurements for clean representative sediment samples from the site with constant water conductivity (σ_w = 0.051 S/m ± 0.001 as NaCl solution) and different water saturations ranging from S_w = 0.58 to S_w = 1.00. To accomplish this, the columns were initially dry packed and then fully saturated. After taking the measurement at full saturation, we drained a specific volume of water from the column using a syringe pump and related this drained volume to the total volume. For testing the effect of the fluid conductivity, we acquired complex conductivity measurements for fully saturated sand samples with different water conductivities, as NaCl solution, ranging from σ_w=0.025 S/m to σ_w=0.098 S/m. This range of fluid conductivities is representative of the samples that we retrieved from the site, which ranged from σ_w=0.025 S/m within the uncontaminated locations to σ_w=0.075 S/m within the contaminated locations.

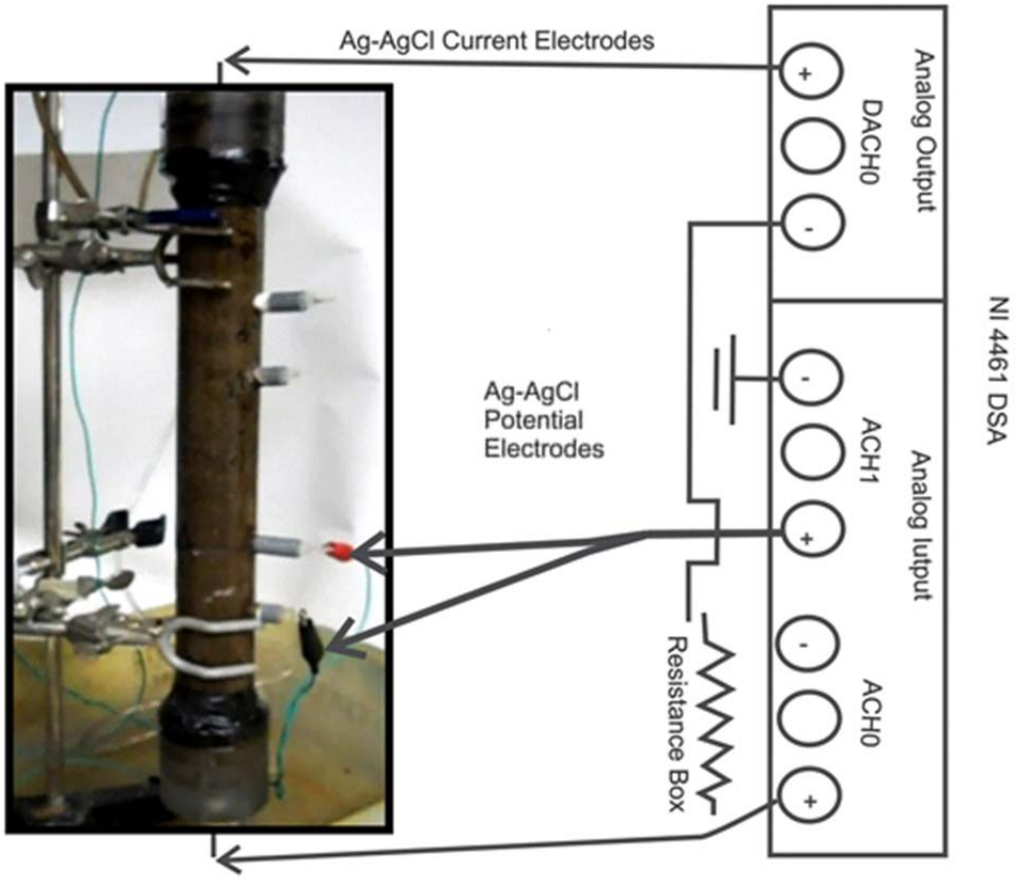

Figure 2. National Instruments 4461 dynamic signal analyzer used for complex conductivity measurements using Ag-AgCl electrodes along the sides of the column.

3.5.4.2. Complex conductivity signatures associated with presence of magnetite

To study the effect of magnetite (as a key biometallic mineral phase at the site) on the complex conductivity response, we acquired complex conductivity measurements over the frequency range 0. 1-1000 Hz for clean sand mixed with different concentrations of magnetite (0.5-5 $mg_{magnetite}/g_{sand}$) spanning the range of magnetite concentration (1.1-4.39 mg/g) found within the sediments retrieved from the site (Mewafy et al., 2011). The magnetite that we used in this experiment was prepared by crushing a magnetite ore

composed of about 95 % magnetite. The grain size for the magnetite ranged from 37 to 270 μm, representing roughly the grain size range of the magnetite at the field site (~50-275 μm). All the samples were fully saturated with NaCl solution (σ_w=0.025 S/m) representing the conductivity of the uncontaminated groundwater within the site.

Another laboratory experiment was conducted to investigate the effect of biometallic mineral (e.g., magnetite) on the complex conductivity response of sediments partially saturated with degraded oil from the site in the presence and absence of magnetite. The degraded oil was collected from the north plume. We first mixed the oil with the sand sample from the site (creating oil wet sand), then the NaCl solution was added and finally the magnetite was added. After this the sand was mixed to a homogeneous state. We measured the complex conductivity response in the frequency range 0.001-1000 Hz for a degraded oil-wet sample (1:1 NaCl solution to degraded oil saturation) before and after the addition of 0.1% by weight of magnetite.

3.6. RESULTS

3.6.1. Complex Conductivity Measurements for Bemidji Cores

We separate our results into saturated (for samples obtained from core segments at or below the average water table) and unsaturated measurements (for samples obtained from core segments within the vadose zone). Figure 3 shows the complex conductivity sampling locations and hydrocarbon distribution along the 2010 and 2011 cores. Figures 4 and 5 show the imaginary and real conductivity for the saturated core segments respectively while Figures 6 and 7 show the same for the unsaturated core segments. The difference in magnitude for the cores retrieved from the free phase plume in 2010 and

2011 can be related to the fact that we saturated 2010 cores; however the general trend show high response for contaminated versus uncontaminated.

3.6.2. Complex conductivity data along saturated cores

The complex conductivity of saturated cores exhibits a higher imaginary conductivity at lower frequency for contaminated samples compared to uncontaminated samples (Figure 4a). In addition, the imaginary conductivity of the saturated contaminated samples is higher for the smear zone samples containing the zone of floating oil compared to the saturated zone samples where the oil is in the dissolved phase (Figure 4b). The σ'' data also show a well-defined relaxation peak centered at 0.01 Hz for the smear zone. The σ' for saturated cores show a similar pattern to the σ'' results, with the highest σ' values observed for samples from within the smear zone compared to the uncontaminated (Figure 5a) and dissolved (Figure 5b) zone samples.

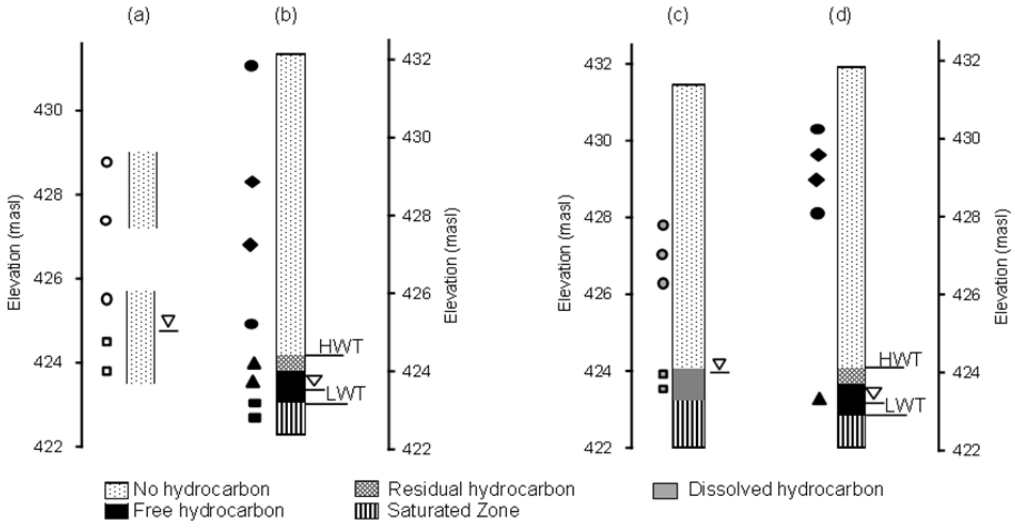

Figure 3. Complex conductivity sampling locations and hydrocarbon distribution along the 2010 uncontaminated (a) and contaminated (b) cores as well as 2011 contaminated cores from dissolved (c) and free (d) phase plume. HWT: Highest water

level, LWT: Lowest water level and HWT: Highest Water Table. Triangle represents water table elevation during the time of measurements. Elevation in meter above sea level (masl).

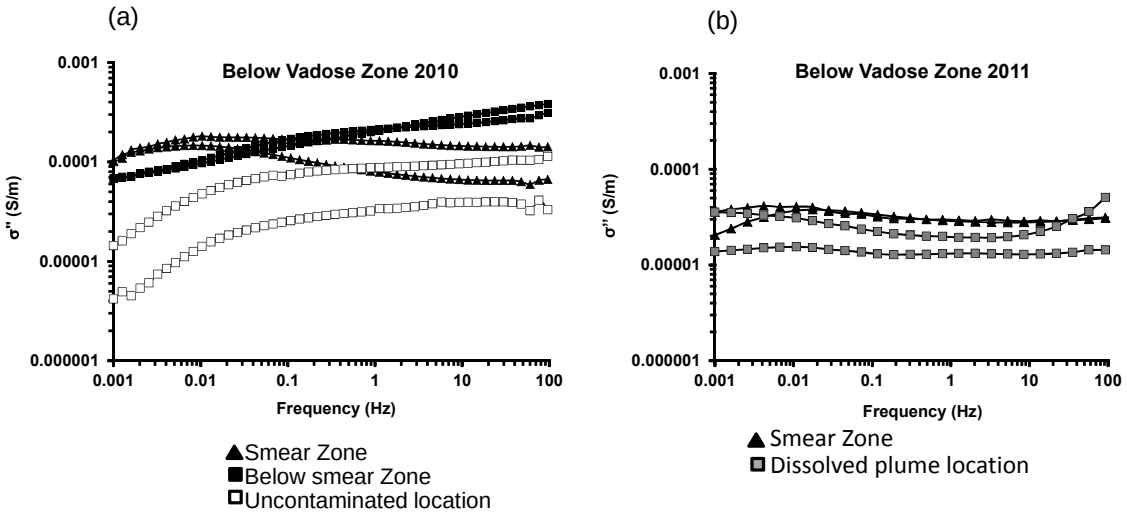

Figure 4: Imaginary conductivity (σ″) for samples retrieved in (a) 2010 from the free phase (FP) plume location (black filled triangles and squares) and the uncontaminated (UC)location (opened squares)and in (b) 2011 from free phase plume (filled triangles) and dissolved phase (DP) plume (grey squares). Note: we divided the zone below the vadose zone in 2010 to smear zone (filled triangles) and below smear zone (filled squares).

3.6.3. Complex conductivity data along unsaturated cores

There is more variability in the data from the unsaturated zone samples where we can observe enhancement in the σ″ data for samples from the vadose zone above the free product plume while the rest are indistinguishable from the uncontaminated samples (Figure 6 a) or dissolved phase plume samples (Figure 6b). For the unsaturated cores,

some samples from the vadose zone above the free phase plume show higher σ′ compared to samples from the vadose zone above the uncontaminated zone (Figure 7a) and above the dissolved phase plume (Figure 7b).

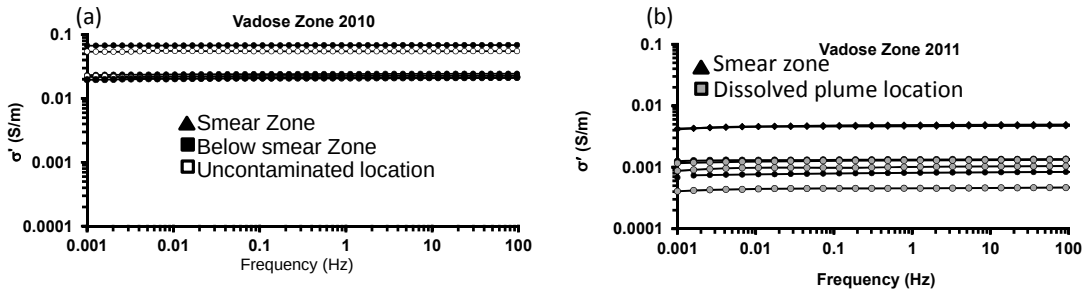

Figure 5: Real conductivity (σ′) for samples retrieved in (a) 2010 from the free phase plume (FP) location (black filled triangles and squares) and the uncontaminated (UC) location (opened squares) and in (b) 2011 from free phase plume (filled triangles) and dissolved phase (DP) plume (grey squares). Note: we divided the zone below the vadose zone in 2010 to smear zone (filled triangles) and below smear zone (filled squares).

3.7. CONTROL EXPERIMENTS

3.7.1. Complex conductivity signatures associated with water saturation and water conductivity

Figure 8 shows the dependency of the real and imaginary conductivity at 1 Hz on fluid conductivity and water saturation. We used equation 3 to model real conductivity at 1 Hz as a function of the fluid conductivity. Figure 8a shows that the imaginary conductivity is less dependent on fluid conductivity and fluid saturation than real conductivity, where

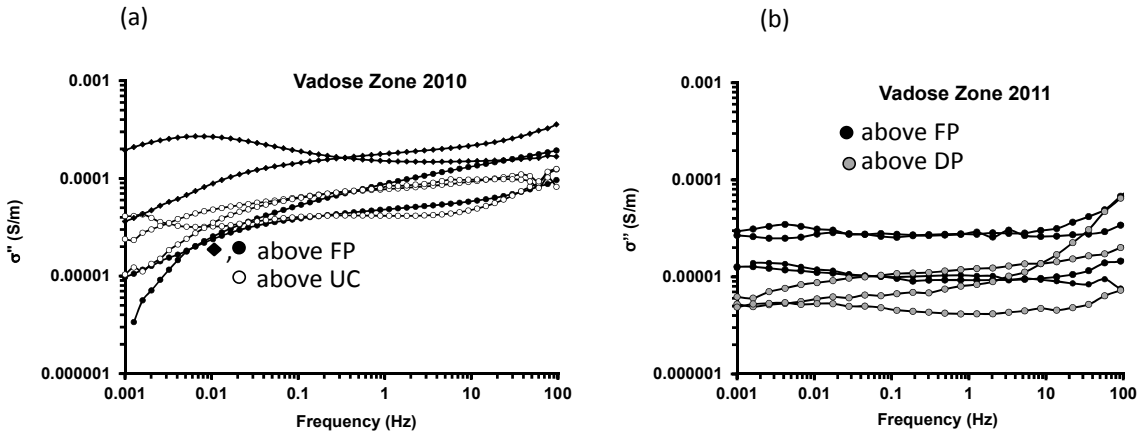

Figure 6: Imaginary conductivity (σ″) along samples retrieved in 2010 (a) above free phase (FP) plume (filled circles and diamonds) and uncontaminated (UC) location (open circles) and in 2011 (b) above free phase(FP) plume (filled circles) and dissolved phase (DP) plume (open triangles).

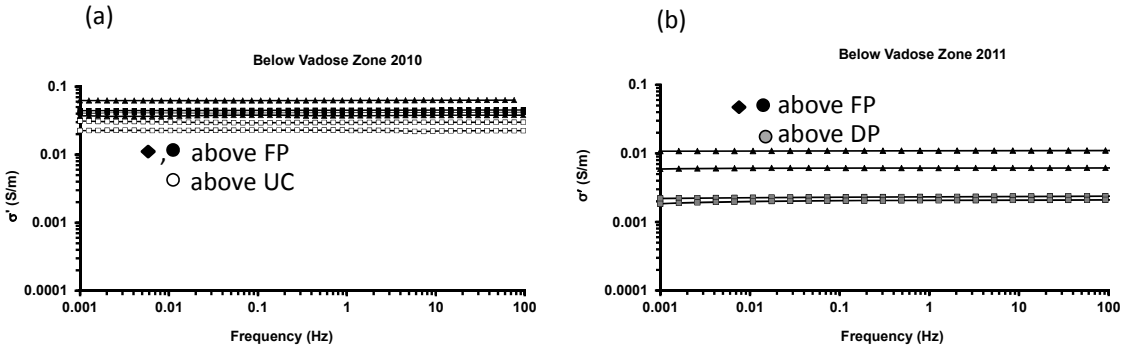

Figure 7: Real conductivity (σ′) along samples retrieved from the vadoze zone in 2010 (a) above free phase (FP) plume (filled circles and diamonds) and uncontaminated (UC) location (open circles) and in 2011 (b) above free phase(FP) plume (filled circles and diamonds) and dissolved phase (DP) plume (grey circles).

real conductivity varies by two orders of magnitude with a formation factor of 7.8 and a surface conductivity of $5*10^{-5}$ (S/m), obtained from the least square regression. The fluid

saturation data shows a strong relationship for real conductivity and a weaker relationship for imaginary conductivity (Figure 8b).

3.7.2. Complex conductivity signatures associated with the presence of magnetite

Figure 9a shows the dependency of σ′ and σ″ at 1 Hz on magnetite content.The magnetite concentration we used in this experiment ranges between 1-7 $mg_{magnetite}/g_{sand}$ to representing the range encountered in the field. We observe that σ″ is highly dependent on magnetite content, where σ″ changes within two orders of magnitude, while the magnitude of σ′ changes within less than one order of magnitude (Figure 9). This large change in σ″ relative to σ′ is evident from the power law exponent, being less for σ′ (~0.091) when compared to σ″ (~0.78), which indicates that variations in magnetite content as documented with the controlled experiment play a major role in the changes in σ″.

Figure 9b and c show the changes in σ″ and σ′ for degraded oil wet samples with and without magnetite. The addition of magnetite to the degraded oil wet sample enhances σ″ by 30% (Figure 9b) and σ′ by 27% (Figure 9c) compared to a degraded oil wet sample without magnetite. The σ″ spectrum of the degraded oil wet sample with magnetite shows a broad relaxation peak between 0.001 and 0.1 Hz (Figure 9c).

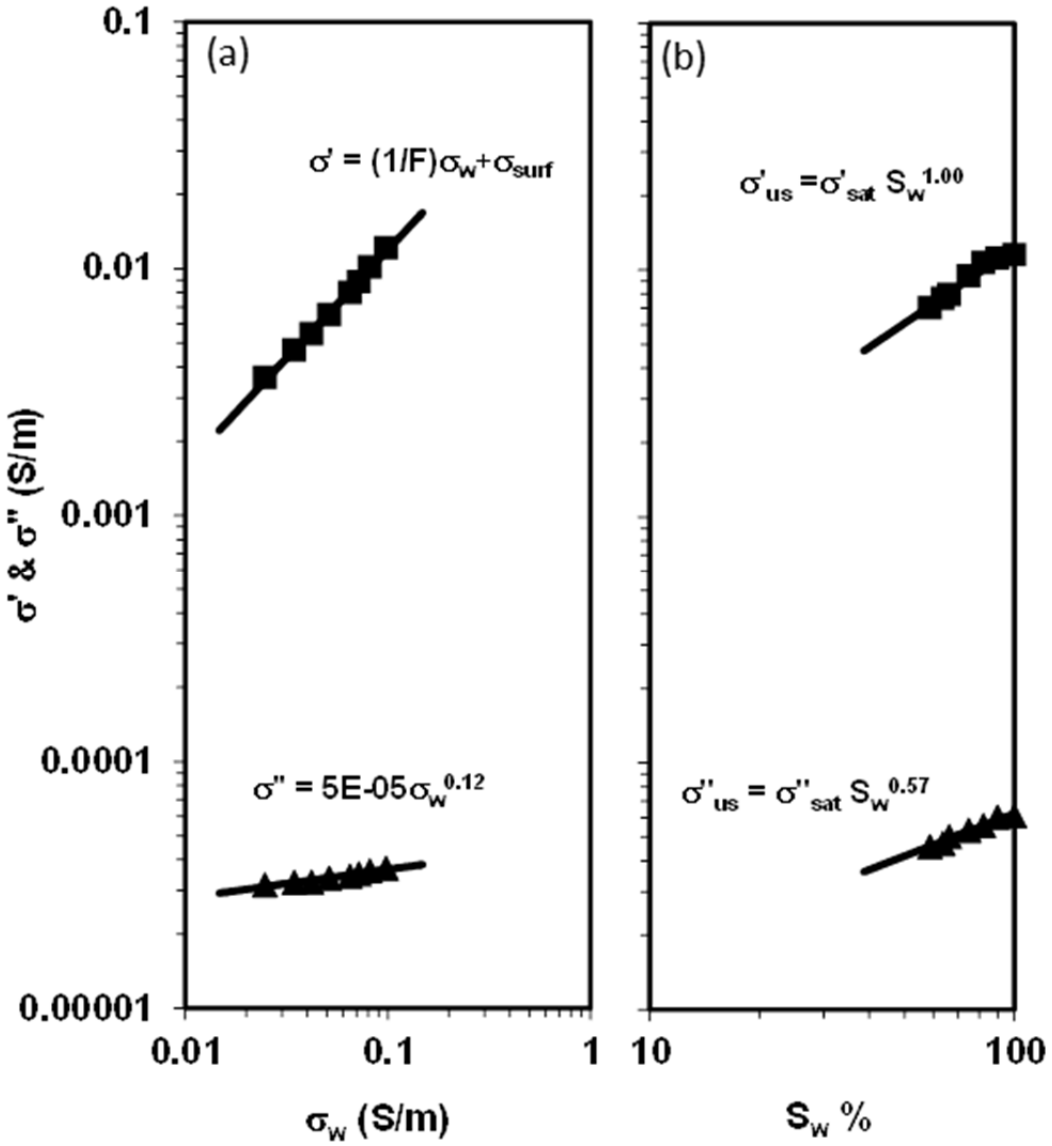

Figure 8: Dependence of the real conductivity (σ′) and imaginary conductivity (σ″) at 1 Hz on (a) fluid conductivity (σ_w) and (b) water saturation (S_w). The data shown include the calculated formation factor of 7.8 and a surface conductivity of $5*10^{-5}$(S/m) obtained from the least square regression.

3.8. DISCUSSION

3.8.1.Variability in the complex conductivity response from field and laboratory measurements

Four three out of four samples investigated, both the σ'' and σ' for samples from the smear zone (in which free product occurs) shows a higher magnitude compared to samples from either the dissolved plume as well as the uncontaminated location (Figures 4 and 5). This observation is not true for the vadose zone samples (Figures 6 and 7) where some samples from the vadose zone above the free product plume show enhancement in the σ'' while the rest are indistinguishable from the uncontaminated samples (Figure 6 a) or dissolved phase plume samples (Figure 6b). These results are consistent with previous observations by Abdel Aal et al. (2004; 2006) indicating a higher imaginary conductivity for contaminated samples especially from the smear zone compared to uncontaminated samples. Abdel Aal et al. (2004, 2006) attributed this enhancement in polarization to the accumulation of microbial cells and/or biofilms with high surface area at the mineral-electrolyte interface (see Revil et al., 2012b for a description of the physics of this process). Abdel Aal et al. (2006) also observed higher imaginary conductivity response for samples in the vadose zone above the contaminated locations not observed at the uncontaminated locations. They speculated that the enhancement in polarization for the vadose zone samples above the free product plume could be related to biodegradation of the vapor phase hydrocarbon emanating from the free phase hydrocarbon below. We offer below an alternative explanation for the enhancement in polarization within the smear zone and within the vadose zone of the free product plume based on results from our control experiments.

3.8.2.Effect of bio-metallic mineral precipitation and dissolved iron on the complex conductivity response

In our control experiments, we tested the effect of other factors that can play a role in the complex conductivity response including the variations in (1) the fluid conductivity, (2) the fluid saturation, and (3) the content of magnetite as an example of bio-metallic mineral. The variation in the pore water conductivity and saturation between samples is unlikely to explain our complex conductivity observations. Control experiments show that the imaginary conductivity is less dependent than the real conductivity on the pore water conductivity and saturation for samples from our field site. Figure 8 shows that the imaginary conductivity changes within less than a half order of magnitude while the real conductivity changes from more than a half order for different saturations to about one order of magnitude for fluid conductivity ranges respectively. This finding is consistent with previous studies (Abdel Aal, et al., 2006). Furthermore, contaminated samples from the vadose part of the smear zone exhibit the highest imaginary conductivity compared to the effect of saturation in our controlled experiment.

To consider the effect of bio-metallic minerals, we conducted two controlled experiments to study the effect of magnetite on the complex conductivity response. Our data shows a significant increase in the magnitude of the imaginary conductivity with increase in magnetite content relative to the real conductivity. Indeed, the power law exponent is much smaller for the real conductivity (~0.015) than for the imaginary conductivity (~1.51) for σ'' (Figure 9a). This experiment indicates that the presence of magnetite within the range of concentrations found at our field site strongly enhances the imaginary conductivity response of porous sediments. Furthermore, as illustrated in Figures 9b and c, the addition of magnetite (0.1% by weight) to degraded oil samples

retrieved from the site resulted in an enhancement of 30% and 27 % in the σ″ and σ′response respectively (between 0.01-0.1 Hz), when compared to degraded oil samples without magnetite. In addition, the σ″ spectrum of the degraded oil wet sample with magnetite shows a broad relaxation peak in the frequency range 0.001-0.1 Hz (Figure 9c). This broad relaxation peak is consistent with some of our results observed for core samples (Figure 4a). At the lower frequencies (between 0.01-0.1 Hz) we clearly differentiate between contaminated and uncontaminated samples.

Magnetic susceptibility (MS) measurements on the cores retrieved from the free product plume locations show two main zones of elevated MS for the contaminated cores: the smear zone (between 423 and 424.5 m elevation) and the vadose zone (between 428 and 430 m elevation) (Figure 10a and b). No enhanced MS zones are observed for the uncontaminated core (Figure 10 c and d). The zones of enhanced MS are coincident with higher iron mineral content (Mewafy et al., 2011). X-ray diffraction confirmed that siderite and magnetite were the dominant iron mineral phases present (see Mewafy et al., 2011 for more details regarding the XRD data). This finding is consistent with previous geochemical studies at the site that have reported the presence of siderite and magnetite associated with microbial transformation of iron (Tuccillo et al., 1999). Nevertheless, of the two minerals, magnetite, which exhibits ferrimagnetism, is largely responsible for the MS response. When compared to siderite, magnetite is also electronically conductive (Odziemkowski et al., 1998). Previous biogeophysical investigations have demonstrated that metallic biominerals have a significant impact on the complex conductivity response due to the enhancement of electrode polarization. (e.g., Williams et al., 2005, 2009; Slater et al., 2007; Personna et al., 2008). Given the

fact that the zones of enhanced complex conductivity show high values of MS, therefore, we postulate that the presence of electronically conductive magnetite can be used to explain the variations that we observe in the complex conductivity response within the contaminated zones at the Bemidji site.

To further explore this point, we plotted the imaginary conductivity (at 0.01Hz) versus the MS for 2010 contaminated and uncontaminated cores (Figure 11). We observed a strong relationship for the contaminated core (R^2=0.85) while the uncontaminated core shows a weaker relationship (R^2=0.48). The weaker correlation for the uncontaminated core can be due to the fewer number of data points. Therefore it is reasonable to assume that the higher σ'' response within the hydrocarbon smear zone is the result of the higher magnetite content. In addition, geochemical data at the site shows that dissolved iron(II) concentrations (~ 40 mg/L) are highest within the oil plume when compared to the dissolved phase plume (less than 0.4 mg/L) or background location (Cozzarelli et al., 2001). Dissolved iron(II), in contrast to the majority of ions in groundwater, is an electroactive ion that can contribute to increasing the charge transfer across the fluid-mineral interface by lowering the charge transfer resistance (Wong, 1979; Williams et al.,2009). The charge transfer resistance also decreases as the concentration of electroactive ions increases (Allen and Larry, 2001).

This is consistent with a recent study at a uranium contaminated site near Colorado, USA where Flores Orozco et al. (2011) used complex conductivity to assess the biogeochemical processes associated with bioremediation of uranium during stimulation of iron- and sulfate-reducing microorganisms. Their data showed spatiotemporal changes in the phase response of aquifer sediments, which correlated with

increases in Fe(II) and precipitation of metal sulfides (e.g., FeS) following the stimulation of iron- and sulfate-reducing bacteria. This study documented a strong correlation between high concentrations of Fe(II) and the imaginary conductivity concomitant with the periods dominated by iron reduction where the concentrations of Fe(II) were above a threshold value of ~ 50μM. However, for periods when sulfate-reduction was the dormant terminal electron acceptor process, the concentration of electroactive Fe(II) was lower (below the critical concentration of 50 μM for their study) and the electrode polarization was minimized and other polarization mechanisms, such as electrochemical or membrane polarization, dominated the SIP response. Flores Orozco et al. (2011) underscores the important role of electroactive ions such as Fe (II) in enhancing the polarization of biometallic minerals. Thus the variability of magnetite content and the concentration of dissolved iron(II), within our site, between the free phase plume and the dissolved plume or the background locations can explain the higher complex conductivity response for the free phase plume. This demonstrates that the Fe(II) concentrations play a very important role in 1) enhancing the polarization and 2) promoting the precipitation of magnetite (Hansel et al., 2003). If magnetite controls the complex conductivity, this may explain the higher σ'' of the vadose zone samples above the free product zone where the elevated zone of MS in the vadose zone (between 428 and 430 m elevation) suggests the presence of magnetite. This provides a reasonable explanation for similar observations from the vadose zone for the Abdel Aal et al. (2006) study.

This has significant implications for our interpretation of geophysical signatures from hydrocarbon contaminated sites. For example, several studies have documented the presence of a zone of enhanced bulk conductivity across the water table interface within

the smear zone and attributed this to increase in pore water conductivity resulting from leaching of aquifer solids due to acid production from microbial activity (e.g., Atekwana et al., 2000; Werkema et al., 2003; Atekwana et al., 2004a-c). Here we hypothesize that the enhancement in bulk conductivity could also be related to the presence of bio-metallic mineral phases in addition to the effect of active ions. However, more work is needed to confirm this hypothesis.

We propose below a new conceptual model summarized in Figure 12. Abdel Aal et al. (2006) suggested a conceptual model for the different factors that enhance the complex conductivity response due to hydrocarbon degradation including mineral weathering enhancement as a result of organic acids production by bacteria and the attachment of microbial cells to mineral surfaces (Figures 12 a and b). These two factors can result in changes in surface area and/or pore constrictions and therefore enhance the complex conductivity response. Here we suggest a modification of this conceptual model where iron reducing bacteria within the anoxic part of the plume reduce ferrihydrite (Figure 12a), resulting in the release of dissolved iron(II). High production rates of iron(II) due to excess organic carbon in the oil pool layer can result in a high iron(II)/ferrihydrite ratio (Figure 12b). Studies by Hansel et al. (2003, 2005) have documented that magnetite and siderite can be formed by the direct sorption of iron(II) to the ferrihydrite under high iron(II) concentrations greater than 3mM. Thus, magnetite coats the sand grains resulting in the enhancement of electrode polarization and microbial attachment within these zones (Figure 12c).

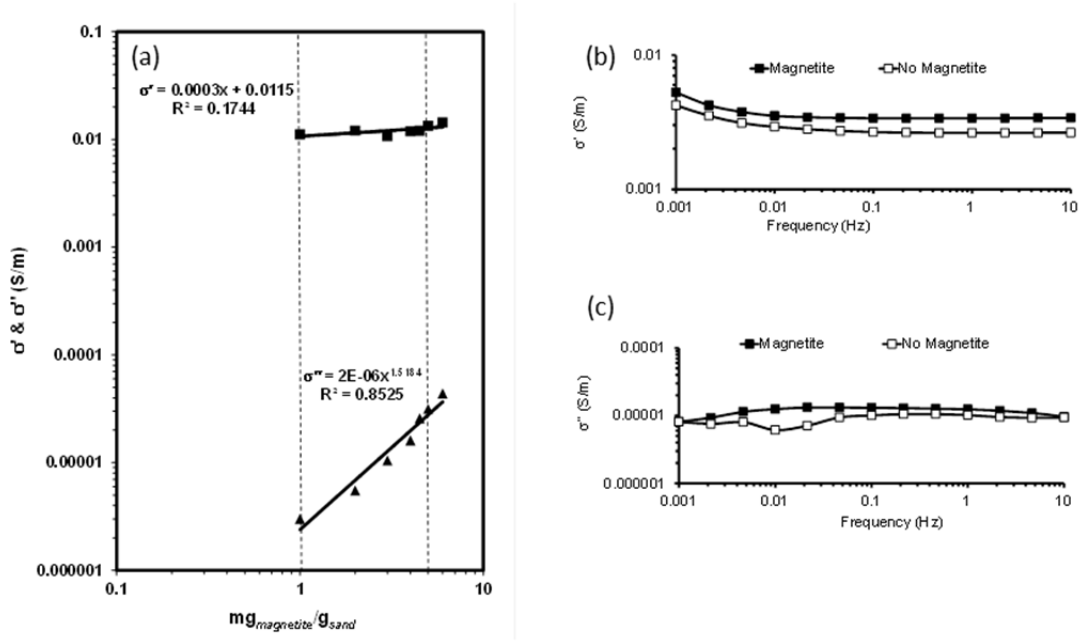

Figure 9: Dependence of the real conductivity (σ′) and imaginary conductivity (σ″) at 1 Hz on magnetite content (a) and on degraded oil with/without magnetite (b, c). The two vertical dashed lines indicate the minimum and maximum magnetite concentration ($mg_{magnetite}/g_{sand}$) for the core samples retrieved from the site.

3.9. CONCLUSIONS

We investigated the complex conductivity response of oil contamination at a site undergoing active bioremediation where iron reduction is the dominant terminal electron process. The magnitude of the real and imaginary conductivity responses is higher for most of samples from the smear zone (where the oil saturation is greatest) compared to the dissolved phase saturated zone where the oil saturation is lower. Saturated zones of enhanced complex conductivity responses are concomitant with zones of high concentration of dissolved iron(II) and enhanced magnetic susceptibility suggesting that the complex conductivity response is driven by the presence of active ions and metallic

bio-iron mineral phases such as magnetite resulting from the microbial oxidation of the hydrocarbons coupled to iron reduction. Also unsaturated zones of enhanced complex conductivity responses are concomitant with zones of enhanced magnetic susceptibility suggesting that the complex conductivity response is driven by the presence metallic bio-iron mineral phases. Thus we suggest that the presence of dissolved iron(II) and/or

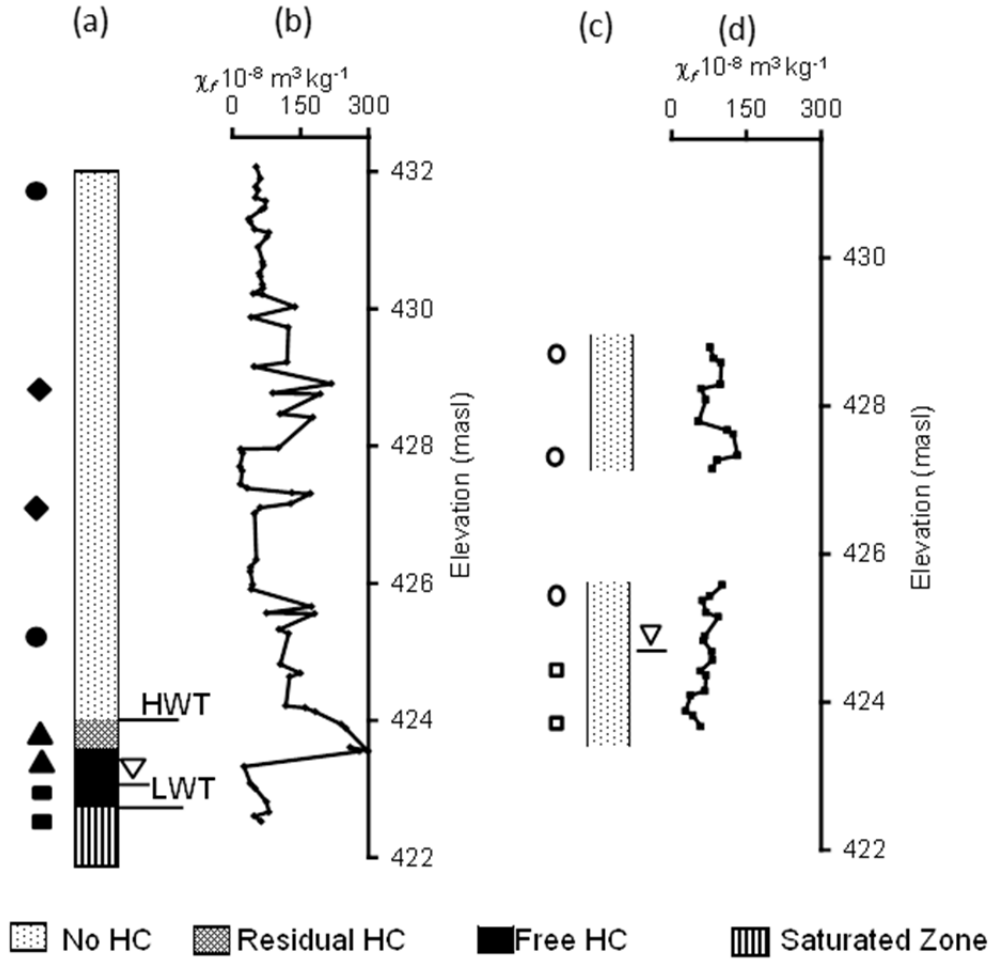

Figure 10: Hydrocarbon distribution (a, c) and laboratory mass magnetic susceptibility (b, d) for 2010 contaminated and uncontaminated cores respectively (Figure modified from Mewafy et al., 2011).

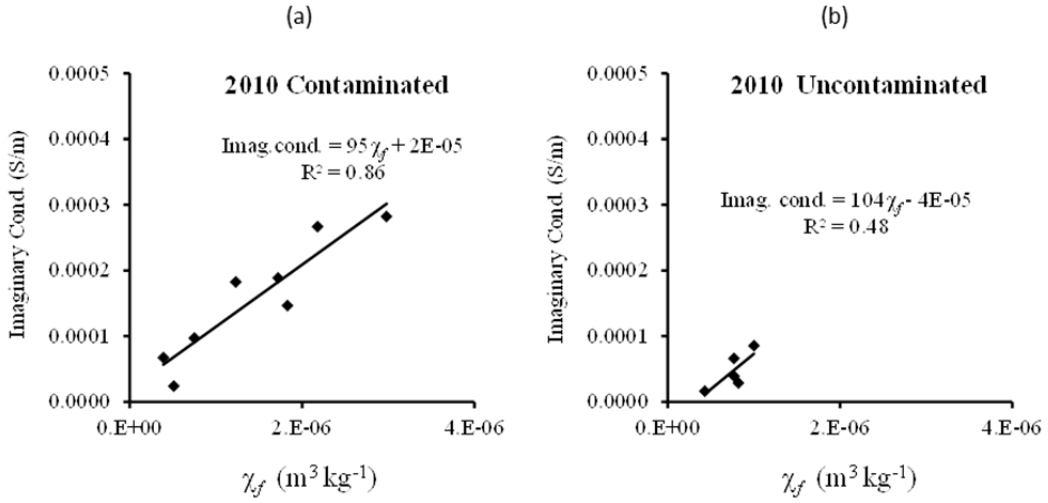

Figure 11: Imaginary Conductivity versus magnetic susceptibility for 2010 contaminated (a) and uncontaminated (b) cores.

metallic biominerals (like magnetite) play a role in enhancing the complex conductivity response within hydrocarbon contaminated sites that have iron reduction as the predominant bio-physicochemical process. This important finding can be used to explain electrical conductivity and complex conductivity data previously observed at other hydrocarbon contaminated sites. Therefore interpreting geophysical data acquired at a hydrocarbon or organic contaminated site has to be guided by the biogeochemical data of that site. This study improves our understanding of the complex conductivity mechanisms within oil contaminated sediments and may pave the way to more accurate interpretations of complex conductivity results from oil contaminated sites.

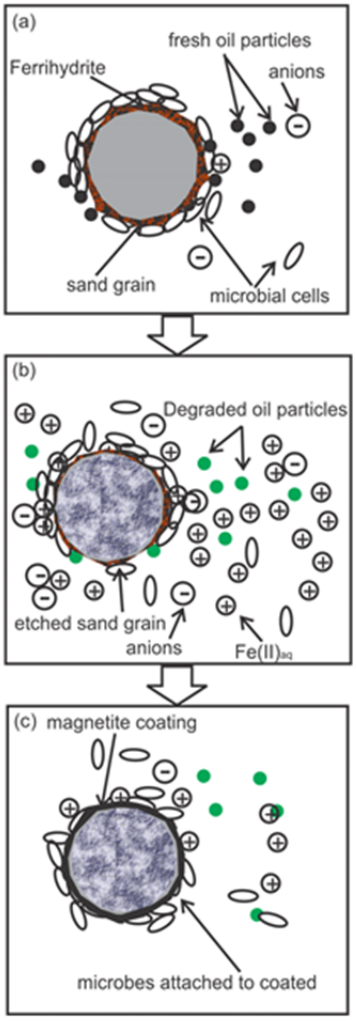

Figure 12: Role of the bacteria reducing ferrihydrite. (a) These bacteria results in the release of dissolved iron(II) and hence an increase of iron(II)/ferrihydrite ratio. (b) This process leads to iron hydroxide precipitation as magnetite coating sand grains. (c). Dissolved iron(II) can enhances complex conductivity as an active ion (Wong, 1979), while Magnetite coating enhances the complex conductivity response directly by electrode polarization and indirectly by altering the surface area (Slater et al., 2006) and enhancing microbial attachment (Abdel Aal et al., 2009).

3.10. REFERENCES

Abdel Aal, G. Z., Atekwana, E. A., Slater, L. D. and Atekwana, E. A., 2004. Effects of microbial processes on electrolytic and interfacial electrical properties of unconsolidated sediments: Geophysical Research Letters, 31, L12505, doi:10.1029/2004GL020030.

Abdel Aal, G.Z.A., Atekwana, E.A. and Slater, L.D., 2006. Induced-polarization measurements on unconsolidated sediments from a site of active hydrocarbon biodegradation, Geophysics, 71(2), H13-H24 .

Abdel Aal, G. Z., Atekwana, E. A., Rossbach, S. and Werkema, D. D., 2010. Sensitivity of geoelectrical measurements to the presence of bacteria in porous media, Journal of Geophysical Research, 115, G03017, doi:10.1029/2009JG001279.

Allen, J. B., and Larry, R. F., 2001. Electrochemical methods: fundamentals and applications: Department of Chemistry and Biochemistry University of Texas at Austin, John Wiley & Sons, Inc.

Allen, D. A., 2008. A review of geophysical equipment applied to groundwater and soil investigation, Report to the Australian National Committee on Irrigation and Drainage, Mawson, Australia.

Archie, G.E., 1942. The electrical resistivity log as an aid in determining some resevoir characteristics, Transactions of the American Institute of Mining Metallurgical Engineers., 146, 54–62.

Atekwana, E., and Atekwana, E., 2010. Geophysical Signatures of Microbial Activity at Hydrocarbon Contaminated Sites: A Review, Surveys in Geophysics, 31(2), 247-283.

Atekwana, E.A., and Slater, L.D., 2009. Biogeophysics: A new frontier in earth science research Reviews of Geophysics, 47, RG4004, doi:10.1029/2009RG000285.

Atekwana, E.A., Atekwana, E., Legall, F.D. and Krishnamurthy, R.V., 2004a. Field evidence for geophysical detection of subsurface zones of enhanced microbial activity, Geophysical Research Letters, 31(23) , doi:10.1029/2004GL021576..

Atekwana, E.A., Rowe, R.S., Werkema, D.D. and Legall, F.D., 2004b. The relationship of total dissolved solids measurements to bulk electrical conductivity in an aquifer contaminated with hydrocarbon, Journal of Applied Geophysics, 56(4), 281-294.

Atekwana, E.A., Werkema, D.D., Duris, J.W., Rossbach, S., Sauck,W.A., Cassidy, D.P., Means, J. and Legall, F.D., 2004c. In-situ apparent conductivity measurements and microbial population distribution at a hydrocarbon-contaminated site, Geophysics, 69(1), 56-63.

Baedecker M. J., Cozzarelli, I. M., Evans, J. R. and Hearn, P. P., 1992. Authigenic mineral formation in aquifers rich in organic material. In Water-Rock Interaction (eds. Y. K. Kharaka and A. S. Maest), pp. 257–261. Balkema.

Baedecker, M.J., Cozzarelli, I.M., Eganhouse, R.P., Siegel, D.I. and Bennett, P.C., 1993. Crude-oil in a shallow sand and gravel aquifer.3. Biogeochical reactions and mass-balance modeling in anoxic groundwater, Applied Geochemistry, 8(6), 569-586.

Bazylinski, D.A., and Frankel, R.B., 2003. Biologically controlled mineralization in prokaryotes, in Biomineralization, edited by P. M. Dove, J. J. DeYoreo and S. Weiner, pp. 217-247.

Bekins, B.A., Cozzarelli, I.M., Godsy, E.M., Warren, E., Essaid, H.I. and Tuccillo, M.E., 2001. Progression of natural attenuation processes at a crude oil spill site: II. Controls

on spatial distribution of microbial populations, Journal of Contaminant Hydrology, 53(3-4), 387-406.

Bennett, P.C., Siegel, D.E., Baedecker, M.J. and Hult, M.F., 1993. Crude-oil in a shallow sand and gravel aquifer.1. Hydrogeology and inorganic geochemistry, Applied Geochemistry, 8(6), 529-549.

Binley, A., Cassiani, G., Middleton, R. and Winship, P., 2002. Vadose zone flow model parameterisation using cross-borehole radar and resistivity imaging. Journal of Hydrology, 267, 147–159.

Börner, F., Gruhne, M. and Schön, J., 1993. Contamination indications derived from electrical properties in the low frequency range, Geophysical Prospecting, 41(1), 83-98.

Breede, K., and A. Kemna, 2012. Spectral induced polarization measurements on variably saturated sand-clay mixtures, Near Surface Geophysics, 10(6), 479-489.

Cassidy, D.P., Hudak, A.J., Werkema, D., Atekwana, E.A., Rossbach, S. J., Duris, W., and Sauck, W.A. 2002. In situ rhamnolipid production at an abandoned petroleum refinery, Soil & Sediment Contamination, 11(5), 769-787.

Che-Alota, V., Atekwana, E.A., Sauck, W.A., and Werkema, D.D., 2009. Temporal geophysical signatures from contaminant-mass remediation, Geophysics, 74(4), B113-B123.

Clement, T.P., Hooker, B.S. and Skeen, R.S., 1996. Macroscopic models for predicting changes in saturated porous media properties caused by microbial growth, Ground Water, 34(5), 934-942.

Cozzarelli, I.M., Baedecker, M.J., Eganhouse, R.P. and Goerlitz, D.F., 1994. The geochemical evolution of low-molecular-weight organic-acids derived from the degradation of petroleum contaminants in groundwater, Geochimica Et Cosmochimica Acta, 58(2), 863-877.

Cozzarelli, I.M., Bekins, B.A., Eganhouse, R.P., Warren, E. and Essaid, H.I., 2010. In situ measurements of volatile aromatic hydrocarbon biodegradation rates in groundwater, Journal of Contaminant Hydrology, 111(1-4), 48-64.

Cozzarelli, I.M., Bekins, B.A., Baedecker, M.J., Aiken, G.R., Eganhouse, R.P. and Tuccillo, M.E., 2001. Progression of natural attenuation processes at a crude-oil spill site: 1. Geochemical evolution of the plume, Journal of Contaminant Hydrology, 53(3-4), 369-385.

Delin, G.N., and Herkelrath, W.N., 1999. Long-term monitoring of unsaturated-zone properties to estimate recharge at the Bemidji crude-oil spill site. In: Morganwalp, D.W., Buxton, H.T. (Eds.), U.S. Geological Survey Toxic Substances Hydrology Program—Proceedings of the technical meeting, Charleston, South Carolina, March 8 –12, 1999. U.S. Geol. Surv. Water-Resour. Invest., 99(4018C), 143– 151.

Dillard, L.A., Essaid, H.I. and Herkelrath, W.N., 1997. Multiphase flow modeling of a crude-oil spill site with a bimodal permeability distribution, Water Resources Research, 33(7), 1617-1632.

Eganhouse, R.P., Baedecker, M.J., Cozzarelli, I.M., Aiken, G.R., Thorn, K.A. and Dorsey, T.F., 1993. Crude-oil in a shallow sand and gravel aquifer .2. Organic geochemistry, Applied Geochemistry, 8(6), 551-567.

Essaid, H.I., Bekins, B.A., Herkelrath, W.N. and Delin, G.N., 2011. Crude Oil at the Bemidji Site: 25 Years of Monitoring, Modeling, and Understanding, Ground Water, 49(5), 706-726.

Flores Orozco, A., Kemna, A., Oberdörster, C., Zschornack, L., Leven, C., Dietrich, P., and Weiss, H., 2012. Delineation of subsurface hydrocarbon contamination at a former hydrogenation plant using spectral induced polarization imaging, Journal of Contaminant Hydrology, 136–137(0), 131-144.

Flores Orozco, A. , Williams, K. H., Long, P. E., Hubbard, S. S., and Kemna, A., 2011. Using complex resistivity imaging to infer biogeochemical processes associated with bioremediation of an uranium-contaminated aquifer: Journal of Geophysical Research: Biogeosciences, 116(G03001), doi: 10.1029/2010JG001591.

Hansel, C. M., Benner, S. G., Neiss, J., Dohnalkova, A., Kukkadapu, R. K., and Fendorf, S., 2003. Secondary mineralization pathways induced by dissimilatory iron reduction of ferrihydrite under advective flow: Geochimica Et Cosmochimica Acta, 67(16), 2977-2992.

Hansel, C. M., Benner, S. G., and Fendorf, S., 2005. Competing Fe(II)-induced mineralization pathways of ferrihydrite: Environmental Science & Technology, 39(18), 7147-7153.

Kemna, A., Binley, A., and Slater, L., 2004. Crosshole IP imaging for engineering and environmental applications, Geophysics, 69(1), 97-107.

Leroy, P., Revil, A., Kemna, A., Cosenza, P., and Ghorbani, A., 2008. Spectral induced polarization of water-saturated packs of glass beads, Journal of Colloid and Interface Science, 321(1), 103-117.

Lesmes, D.P., and Frye, K.M., 2001. Influence of pore fluid chemistry on the complex conductivity and induced polarization responses of Berea sandstone, Journal of Geophysical Research-Solid Earth, 106(B3), 4079-4090.

Lovley D. R., Baedecker, M. J., Lonergan, D. J., Cozzarelli, I. M., Phillips, E. J. P., and Siegel, D. I., 1989. Oxidation of aromatic contaminants coupled to microbial iron reduction, Nature, 339, 297– 299.

Lovley, D.R., Stolz, J.F., Nord, G.L., and Phillips, E.J.P., 1987. Anaerobic production of magnetite by a dissimilatory iron-reducing microorganism, Nature, 330(6145), 252-254.

Marshall, D. and Madden, T., 1959. Induced polarization, a study of its causes. Geophysics, 24: 790-816.

Mewafy, F.M., Atekwana, E.A., Werkema, Jr., D.D., Slater, L.D., Ntarlagiannis, D., Revil, A., Skold, M., and Delin, G.N., 2011. Magnetic susceptibility as a proxy for investigating microbially mediated iron reduction, Geophys. Res. Lett., 38(21), L21402.

Nevin, K. P., Holmes, D. E., Woodard, T. L., Hinlein, E. S., Ostendorf, D. W., and Lovley, D. R., 2005. Geobacter bemidjiensis sp. nov. and Geobacter psychrophilus sp. nov., two novel Fe(III)-reducing subsurface isolates, Int. J. Syst. Evol. Microbiol., 55(4), 1667–1674, doi:10.1099/ijs.0.63417-0.

Odziemkowski, M., Schuhmacher, T., Gillham, R., and Reardon, E., 1998. Mechanism of oxide film formation on iron in simulating groundwater solutions: Raman spectroscopic studies: Corrosion Science, 40(2), 371-389.

Olhoeft, G.R., 1985. Low-frequency electrical-properties, Geophysics, 50(12), 2492-2503.

Pelton, W.H., Ward, S.H., Hallof, P.G., Sill, W.R., Nelson, P.H., 1978. Mineral discrimination and removal of inductive coupling with multifrequency IP, Geophysics, 43, 588-609.

Personna, Y.R., Ntarlagiannis, D., Slater, L., Yee, N., O'Brien, M., and Hubbard S., 2008. Spectral induced polarization and electrodic potential monitoring of microbially mediated iron sulfide transformations, Journal of Geophysical Research-Biogeosciences, 113, G02020, doi:10.1029/2007JG000614.

Prommer, H., Davis, G.B., and Barry, D.A., 1999. Geochemical changes during biodegradation of petroleum hydrocarbons: field investigations and biogeochemical modelling, Organic Geochemistry, 30(6), 423-435.

Revil, A., and Glover, P. W. J., 1998. Nature of surface electrical conductivity in natural sands, sandstones, and clays, Geophysical Research Letters, 25, 691–694, doi:10.1029/98GL00296

Revil A., and Florsch, N., 2010. Determination of permeability from spectral induced polarization data in granular media, Geophysical Journal International, 181, 1480-1498, doi: 10.1111/j.1365-246X.2010.04573.x.

Revil, A., Schmutz, M., and Batzle, M.L., 2011. Influence of oil wettability upon spectral induced polarization of oil-bearing sands, Geophysics, 76(5), A31-A36.

Revil, A., Atekwana, E., Zhang, C., Jardani, A., and Smith, S., 2012a. A new model for the spectral induced polarization signature of bacterial growth in porous media, Water Resources Research, 48, W09545, doi:10.1029/2012WR011965.

Revil, A., Koch, K., and Holliger, K., 2012b. Is it the grain size or the characteristic pore size that controls the induced polarization relaxation time of clean sands and sandstones?: Water Resources Research, 48(5), W05602.

Rijal, M.L., Appel, E., Petrovsky, E., and Blaha, U., 2010. Change of magnetic properties due to fluctuations of hydrocarbon contaminated groundwater in unconsolidated sediments, Environmental Pollution, 158(5), 1756-1762.

Rijal, M., Porsch, K., Appel, E., and Kappler, A., 2012. Magnetic signature of hydrocarbon-contaminated soils and sediments at the former oil field Hänigsen, Germany: Studia Geophysica Et Geodaetica, 56(3), 889-908.

Schmutz, M., Blondel, A., and Revil, A., 2012. Saturation dependence of the quadrature conductivity of oil-bearing sands: Geophysical Research Letters, 39(L03402), doi: 10.1029/2011GL050474.

Schmutz, M., Revil, A., Vaudelet, P., Batzle, M., Vinao, P. F., and Werkema, D. D., 2010. Influence of oil saturation upon spectral induced polarization of oil-bearing sands: Geophysical Journal International, 183(1), 211-224.

Slater, L., and Binley, A., 2006. Synthetic & field based electrical imaging of a zerovalent iron barrier: implications for monitoring long-term barrier performance, Geophysics, 71(5), B129-B137.

Slater, L., Ntarlagiannis, D., Personna, Y.R., and Hubbard, S., 2007. Pore-scale spectral induced polarization signatures associated with FeS biomineral transformations, Geophysical Research Letters, 34(21404), doi:10.1029/2007GL031840.

Slater, L.D., and Lesmes, D., 2002. IP interpretation in environmental investigations, Geophysics, 67(1), 77-88.

Thullner, M., Zeyer, J., and Kinzelbach, W., 2002. Influence of microbial growth on hydraulic properties of pore networks, Transport in Porous Media, 49(1), 99-122.

Tuccillo, M.E., Cozzarelli, I.M., and Herman, J.S., 1999. Iron reduction in the sediments of a hydrocarbon-contaminated aquifer, Applied Geochemistry, 14(5), 655-667.

Ulrich, C., and Slater, L. D., 2004. Induced polarization measurements on unsaturated, unconsolidated sands, Geophysics, 69(3), 762-771.

Vanhala, H., Soininen, H., and Kukkonen, I., 1992. Detecting organic chemical contaminants by spectral-induced polarization method in glacial till environment, Geophysics, 57(8), 1014-1017.

Vinegar, H.J., and Waxman, M.H., 1984. Induced polarization of shaly sands, Geophysics, 49(8), 1267-1287.

Waxman, M.H., and Smits, L.J.M., 1968. Electrical conductivities in oil-bearing shaly sands, Society of Petroleum Engineers Journal, 8(2), 107-122.

Werkema, D.D., Atekwana, E.A., Endres, A.L., Sauck, W.A., and Cassidy, D.P., 2003. Investigating the geoelectrical response of hydrocarbon contamination undergoing biodegradation, Geophysical Research Letters, 30(12), 1647, doi:10.1029/2003GL017346.

Williams, K.H., Ntarlagiannis, D., Slater, L.D., Dohnalkova, A., Hubbard, S.S., and Banfield, J.F., 2005. Geophysical imaging of stimulated microbial biomineralization, Environmental Science & Technology, 39(19), 7592-7600.

Williams, K.H., Kemna, A., Wilkins, M.J., Druhan, J., Arntzen, E., N'Guessan, A.L., Long, P.E., Hubbard, S.S., and Banfield, J.F., 2009. Geophysical Monitoring of

Coupled Microbial and Geochemical Processes During Stimulated Subsurface Bioremediation, Environmental Science & Technology, 43(17), 6717-6723.

Wong, J., 1979. An electrochemical model of the induced-polarization phenomenon in disseminated sulfide ores, Geophysics, 44(7), 1245-1265.

PAPER 3

HIGH-RESOLUTION MAGNETIC SUSCEPTIBILITY MEASUREMENTS FOR INVESTIGATING MAGNETIC MINERAL FORMATION DURING MICROBIAL MEDIATED IRON REDUCTION

4.1. ABSTRACT

Disimilatory iron-reducing bacteria play an important role in the reduction of Fe(hydr)oxides and the production of secondary solid-iron mineral phases. Therefore, they have a profound influence on the coupling of the biogeochemical cycles of carbon and iron. These secondary solid-iron mineral phases can have magnetic properties, suggesting that geophysical tools such as magnetic susceptibility can play an important role in identifying zones where microbial-mediated iron mineral transformations are occurring. We investigated the magnetic susceptibility variations in a hydrocarbon-contaminated aquifer where methanogenesis and iron-reduction are the main terminal electron acceptor processes. Our objectives are (1) to provide a detailed picture of the variability of magnetic susceptibility at the field site, (2) to determine the hydrobiogeochemical controls on the magnetic susceptibility variability, and (3) evaluate the use of magnetic susceptibility as a viable technique for identifying zones where biogeochemical cycling of iron and organic carbon is occurring. Magnetic

susceptibility data were acquired down 15 boreholes within contaminated (both free phase and dissolved phase) and uncontaminated locations. Our results show an enhanced zone of magnetic susceptibility ~1-2 m thick at the contaminated locations. These magnetic susceptibility anomalies are not observed at the background locations. Magnetic susceptibility values within the free phase plume are on the average higher (150-290$\times10^{-4}$ SI) compared to values within the dissolved phase plume (70-110$\times10^{-4}$ SI). The zone of magnetic susceptibility enhancement is limited to the zone of water table fluctuations and coincident with high concentrations of dissolved Fe(II) and high organic carbon contents. This suggests that the precipitation of magnetic minerals is related to microbial iron-reduction coupled to the oxidation of hydrocarbon compounds. High magnetic susceptibility values within the vadose zone above the free phase plume is coincident with a zone of methane depletion suggesting aerobic or anaerobic oxidation of methane coupled to iron-reduction. Magnetic susceptibility S can serve as a proxy for intrinsic bioremediation by iron-reducing bacteria and for the application of geophysics to iron and carbon cycling studies.

4.2. INTRODUCTION

Iron is the fourth most abundant element and one of the most dominant redox active metals in the Earth's crust. Microorganisms reduce Fe(III) as ferrihydrite with either organic acids or H_2 as electron donor (Lovley, 1993; Tuccillo et al., 1999). Microbial iron reduction in the presence of organic carbon within sediments can lead to mineral dissolution and weathering, the formation (Chaudhuri et al., 2001; Stumm and Sulzberger, 1992) of magnetite and siderite. Microbial iron reduction results in the formation of biometallic iron mineral phases. Hydrocarbon-contaminated environments

therefore provide excellent natural laboratories for investigating iron mineral transformations and the relationship between carbon and iron cycles. Many studies have documented that iron reducing bacteria can use hydrocarbon as a carbon source to reduce iron(III) to iron(II) (Anderson and Lovley, 2000; Lovley et al., 1989) to form siderite (Fredrickson et al., 1998; Mortimer and Coleman, 1997), magnetite (Lovley, 1990; Lovley et al., 1987; Mortimer and Coleman, 1997; Prommer et al., 1999; Rijal et al., 2010), vivianite (Fredrickson et al., 1998), ferroan calcite (Baedecker et al., 1992), and green rust (Fredrickson et al., 1998; Parmar et al., 2001).

Biomineralizaion pathways for different iron mineral phases are controlled by many factors including pH, redox potential, carbonate concentration, and mostly, respiration-driven Fe(II) supply rate and magnitude (Fredrickson et al., 1998; Zachara et al., 2002). Reaction of Fe(II) with ferrihydrite results in different secondary mineralization pathways including: goethite, lepidocrocite, and magnetite. These phases vary in their precipitation extent, rate, and residence time, all of which are primarily a function of Fe(II) concentration and ligand type (Cl, SO_4, CO_3). While lepidocrocite and goethite precipitate over a wide Fe(II) concentration range, magnetite and siderite accumulation is only observed at surface loadings greater than 1.0 mmol Fe(II)/g ferrihydrite (in the absence of bicarbonate). In a laboratory experiment, Zachara et al. (2002) investigated the biomineralization of poorly crystalline Fe(III) oxides by dissimilatory metal reducing bacteria (DMRB). They observed that the supply rate and total concentration of biogenic Fe(II) are the primary determinants of the nature of secondary mineralization products. At lower supply rates, they observed the precipitation of Fe(III) oxides; while at medium and higher rates, magnetite and siderite were dominant precipitates respectively. Hansel

et al. (2003) and Sumoondur et al. (2008) showed in controlled experiments that, as a function of Fe(II) concentration and ligand type (Cl, SO_4, CO_3), magnetite can be the end-product of a process that may proceed via intermediate phases such as lepidocrocite, goethite, and sulphate green rust. Additionally, Hansel et al. (2005) documented the precipitation of magnetite when the Fe(II)/ferrihydrite ratio is greater than 1.0 mmol Fe(II)/g ferrihydrite. Hansel et al. (2003) observed the formation of goethite and magnetite by sorption of Fe(II) to ferrihydrite.

The bio-metallic minerals, in addition to other iron minerals, show a broad range of magnetic susceptibility (MS) responses between highly positive response for ferrimagnetic minerals such as magnetite (513-1116× 10^{-6} m^3 Kg^{-1}), maghemite (410-440× 10^{-6} m^3 Kg^{-1}) (Dunlop and Özdemir, 2001), and greigite (320× 10^{-6} m^3 Kg^{-1}) (Roberts et al., 2011) to low response such for antiferromagnetic minerals as hematite (1.19-1.69× 10^{-6} m^3 Kg^{-1}), goethite (<1.26× 10^{-6} m^3 Kg^{-1}), siderite (1.0× 10^{-6} m^3 Kg^{-1}), pyrite (0.3× 10^{-6} m^3 Kg^{-1}), and lepidocrocite (0.5-0.75× 10^{-6} m^3 Kg^{-1}) (Dearing, 1994). Thus MS might be used as a tool to diagnose biogeochemical zones where the coupling of carbon and iron cycling is occurring so that they may be more appropriately studied.

MS data from hydrocarbon contaminated sites have documented zones of enhanced MS within the smear zone coincident with the free phase hydrocarbon plume (Mewafy et al., 2011; Rijal et al., 2010; Rijal et al., 2012). These studies suggests that MS can be used as a tool: (1) to infer regions of hydrocarbon contamination, and (2) to investigate intrinsic bioremediation by iron reducing bacteria.

A recent study by Porsch et al. (2010) suggests the use of MS to monitor the mineralogical transformations of iron minerals. The secondary mineralization pathways

for the conversion of ferrihydrite to different iron mineral phases is controlled by the biogeochemical factors in the aquifer including Fe(II)/Fe(III) ratios and pH (Hansel et al., 2003, 2005; Sumoondur et al., 2008). Therefore understanding the biogeochemical controls for the formation of magnetic minerals is critical for the development of MS as a viable technique for elucidating the relationship between carbon and iron cycles.

In present work, we investigated the MS variations at a hydrocarbon contaminated aquifer near Bemidji, Minnesota, where methanogenesis and iron-reduction are the main terminal electron acceptor processes (Baedecker et al., 1993). This site represents a natural laboratory available for investigating biophysicochemical processes associated with the intrinsic bioremediation of a crude oil spill. It is also characterized by an extensive geochemical and biological data base. Our objectives are to: (1) provide a detailed picture of the variability of MS at the field site, (2) determine what controls the variability of the MS and (3) evaluate, using field based research, the use of MS as a viable technique for identifying zones where biogeochemical cycling of iron and organic carbon is occurring.

4.3. SITE HISTORY

The National Crude Oil Spill Fate and Natural Attenuation Research Site at Bemidji, MN (Figure 1), is a natural laboratory available for investigating biophysicochemical processes associated with the intrinsic bioremediation of a crude oil spill (Cozzarelli et al., 2001; Eganhouse et al., 1993). The site geology consists of ~ 20 m-thickness of moderately calcareous silty sand and outwash glacial deposits overlying clayey till of unknown thickness (Bennett et al., 1993). In August 1979, a high pressure crude oil pipeline ruptured, releasing 1,700,000 L of crude oil. Oil pooled in low-topography areas

(~2000 m^2) over a total area of 6,500 m^2 to the southwest of the pipeline, forming the north and south contaminated pools. Our study is located on the north pool as it has been the focus of intensive geochemical (Cozzarelli et al., 2010) and microbiological studies (Bekins et al., 2001). According to Essaid et al. (2011), the north pool has a maximum oil saturation of 0.74 m in the down gradient part of the oil body with a smear zone of more than 2 m. The water table ranges from 0 m (near an unnamed lake) to 11 m depth with ~ 1 m seasonal fluctuation at about 8 m below land surface (Delin et al., 1998).

The uncontaminated groundwater is aerobic with dissolved oxygen concentrations between 8 and 9 mg/L, dissolved organic carbon of 2.8 mg/L as C, and low levels of nitrate at 44.8 μg/L as N_2 and sulfate at 2.9 mg/L (Bennett et al., 1993). Geochemical changes in the plume have been previously described by Baedecker et al. (1993) and Cozzarelli et al. (2010). The aquifer is divided in the vicinity of the oil body into anoxic, transition, and background zones. In the anoxic portion, hydrocarbons are oxidized predominantly by iron reduction (Lovley et al., 1989) and methanogenesis (e.g., Baedecker et al., 1993). Bekins et al. (2001) identified two zones of methanogenic activity with CH_4 concentrations greater than 15 mg/L. The vadose zone vapor plume near the oil body has low O_2 (< 2%) and high CO_2 (>10%) and CH_4 (>15%) levels. Based on the estimation of four physiologic microbial populations: aerobes, iron reducers, heterotrophic fermenters, and methanogens Bekins et al. (2001) observed the progression within the anaerobic portion of the contaminated aquifer from iron-reduction to methanogenesis.

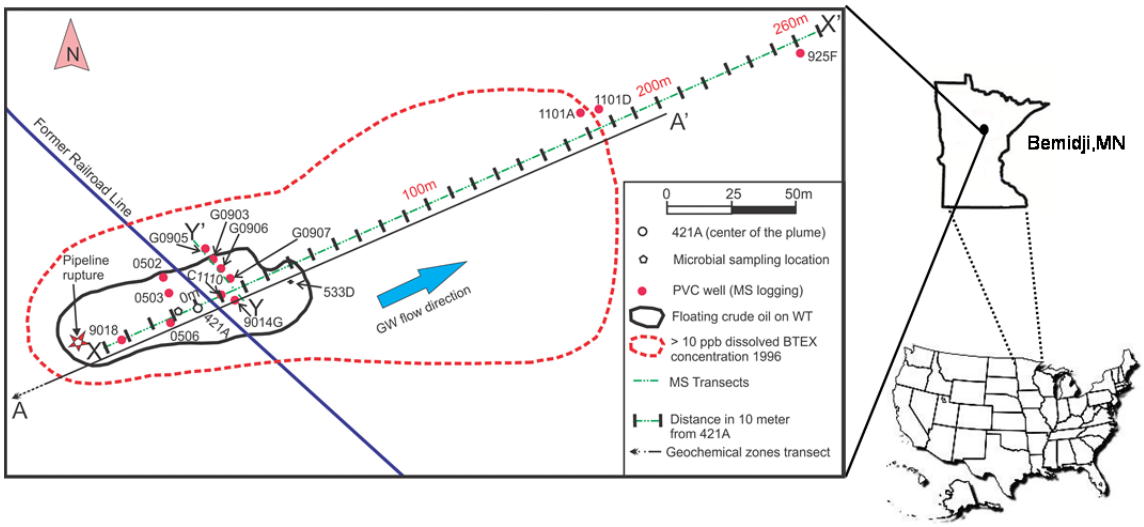

Figure 1: Study site showing location of boreholes and magnetic susceptibility transects X-X' and Y-Y' (shown on figures 3 and 4).

Eight geochemical zones have been identified at the North oil pool (Figure 2), five within the saturated zone (Zones 1-5), and three within the unsaturated zone (Zones 6-8) (Baedecker et al., 1993; Bennett et al., 1993; Delin et al., 1998). Zone 1 is characterized by the uncontaminated oxygenated native ground water. Zone 2 lies beneath the spray zone where the pipeline ruptured and is characterized by low oxygen concentrations and high concentrations of total dissolved inorganic and organic carbon. Zone 3 lies beneath the floating oil within the anoxic plume where the ground water contains high concentrations of hydrocarbons, dissolved manganese (II), iron (II), and methane. Zone 4 is a transition zone from anoxic to oxygenated conditions with low concentrations of hydrocarbons as a result of aerobic degradation processes. Zone 5 shows oxygenated water downgradient from the contamination plume that contains slightly higher concentrations of dissolved constituents, such as benzene, toluene, ethylbenzene, and xylene (BTEX). Zone 6 exhibits near atmospheric concentrations of O_2. Zone 7 denotes a

transition zone with lower concentrations of O_2 (10-20 percent), hydrocarbon concentrations less than 1 part per million (ppm), and higher concentrations of CO_2 (0-10 percent) and CH_4 (0-10 percent). Finally, zone 8 is relatively anoxic and contains maximum concentrations of CO_2 (>10 percent), CH_4 (>10 percent), and hydrocarbon (>1 ppm).

Geochemical and microbial studies suggest iron reduction is an important terminal electron acceptor process occurring within the anaerobic plume (e.g. Baedecker et al., 1993). In addition, iron-reducing bacteria such as *Geobacter bemidjiensis sp*. and *Geobacter psychrophilus sp* occur in this anaerobic plume (Nevin et al., 2005). Several studies have investigated the mineralogy of the sediments within the site (Baedecker et al., 1992; Baedecker et al., 1993; Tuccillo et al., 1999; Zachara et al., 2004). Iron minerals in sediments include goethite, hematite, magnetite, ferrihydrite, and maghemite (Bekins et al., 2001).

4.4. METHODOLOGY

We conducted MS surveys along two, nearly-perpendicular profiles; one in the direction of the groundwater flow, the other nearly perpendicular to the groundwater flow direction. MS data were acquired down 15 boreholes (Figure 1) within contaminated (both free phase and dissolved phase) and uncontaminated locations using a Barington MS probe[*Dearing*, 1994; *Lecoanet et al.*, 1999]. Most of the boreholes have polyvinylchloride (PVC) casings. The Bartington MS probe is 43 mm in diameter, 1.9 meter in length, and operates at a frequency of 1.439 kHz. It is characterized by a vertical resolution of 25 mm and accuracy between 10^{-5} to 1 cgs. The probe is supplied with a test block which is used to check for correct operation of the probe. In this probe, a current is

induced by an oscillating magnetic field at around the probe coils. The oscillating current produces a secondary field that is detected by the receiver coils. The 'in-phase' signal is a measure of the susceptibility of the formations with magnetic properties.

4.5. RESULTS

The variability in MS along the longitudinal profile (X-X′) is shown in Figure 3. The transverse profile (Y-Y′) is shown in Figure 4. In addition, average MS values of the vadose zone (2 m interval above the WT fluctuating zone), the zone of WT fluctuation and below this zone (2 m interval) are presented in Figure 5. In general, we observe an enhanced zone of MS ~1-2 m thick at the contaminated locations. This type of anomaly is not observed at the background locations. Moreover, we observed a unique shape of the MS anomaly as most of the MS anomalies across the site show a gradual increase towards the WT interface, with a harp decrease above the WT. MS values within the free product plume are on the average higher (150-290$\times10^{-4}$ SI) compared to values within the dissolved product plume (70-110$\times10^{-4}$ SI) which are higher than those from the uncontaminated location (~60$\times10^{-4}$ SI).

4.5.1. Vadose Zone

We observe significant variability in the magnitude of the MS values depending on the location with the plume (Figures 3, 4, and 5). Higher MS values (50-150$\times10^{-4}$ SI) are observed in the vadose zone above the free phase plume (9018, 0503, and 9014) corresponding to geochemical zone 8 (Figure 2). While the vadose zone above the dissolved plume shows values of (10-50$\times10^{-4}$ SI) corresponding to geochemical zone 6 (1101a, 1101d, G0905 and G0903) (Figures 3 and 4). The only borehole that deviates

from this trend is G0907 within the free phase plume. Figure 5 shows a correlation of the MS variation between the vadose zone above the free phase and above the dissolved phase plumes for the depth interval between 424-426 m, for boreholes (9018, 0503 and 9014). MS values for this interval are about two to four times higher within the free phase plume (63-99$\times10^{-4}$ SI) compared to (13-28$\times10^{-4}$ SI) for the boreholes within the dissolved plume (see wells 1101a,1101d, G0905, and G0903, Figure 5).

4.5.2. Zone of WT fluctuation

MS values across the site show a marked increase within the zone of WT fluctuation where the zone of enhanced MS straddles the WT interface. This zone extends from the highest water mark to the lowest water mark encompassing the upper part of geochemical zone 3 and the lower part of zones 8 and 7 (Figure 2). The thickness of the enhanced MS zone deceases from ~1.7 m within the free phase plume to ~0.6 m within the dissolved phase plume (Figure 3 and 4). Also, in agreement with (Rijal et al., 2010), most of the MS anomalies show a gradual increase towards the WT interface, and decrease dramatically above the WT interface for wells 9014, G0907, G0906, and G0905 (Figure 4). In addition, we observe a decrease in the magnitude of the MS values downgradient from the free phase plume to the dissolved plume. For example, along profile X-X′ the MS for borehole 9014, which is located about 15 m down gradient (i.e., within the free phase plume) from the center of the plume, has a magnitude peak of about 424$\times10^{-4}$ SI. This high value can be compared to the value recorded in well 1101D (peak at 87.9$\times10^{-4}$ SI). This well is located within the dissolved phase plume (~180 m from the core of the plume) (Figure 3). Also, the average values from within the zone of WT fluctuation (~423-425, along X-X′ and Y-Y′) suggest that this zone of enhanced MS is about four

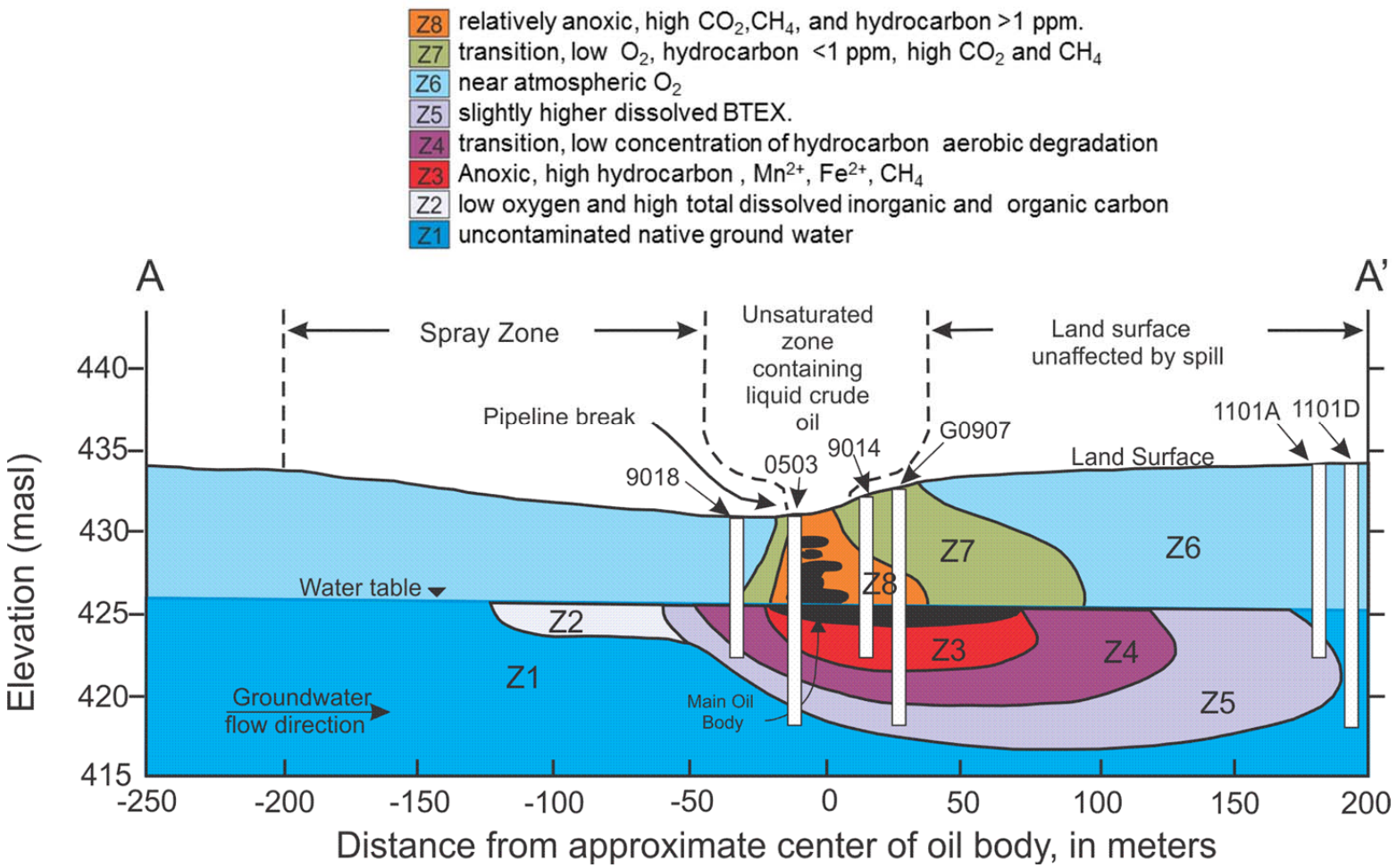

Figure 2: Geochemical zones in the unsaturated and saturated zones at the North oil pool, 1997 [Modified from Delin et al., 1998] across the free phase plume and dissolved phase plume.

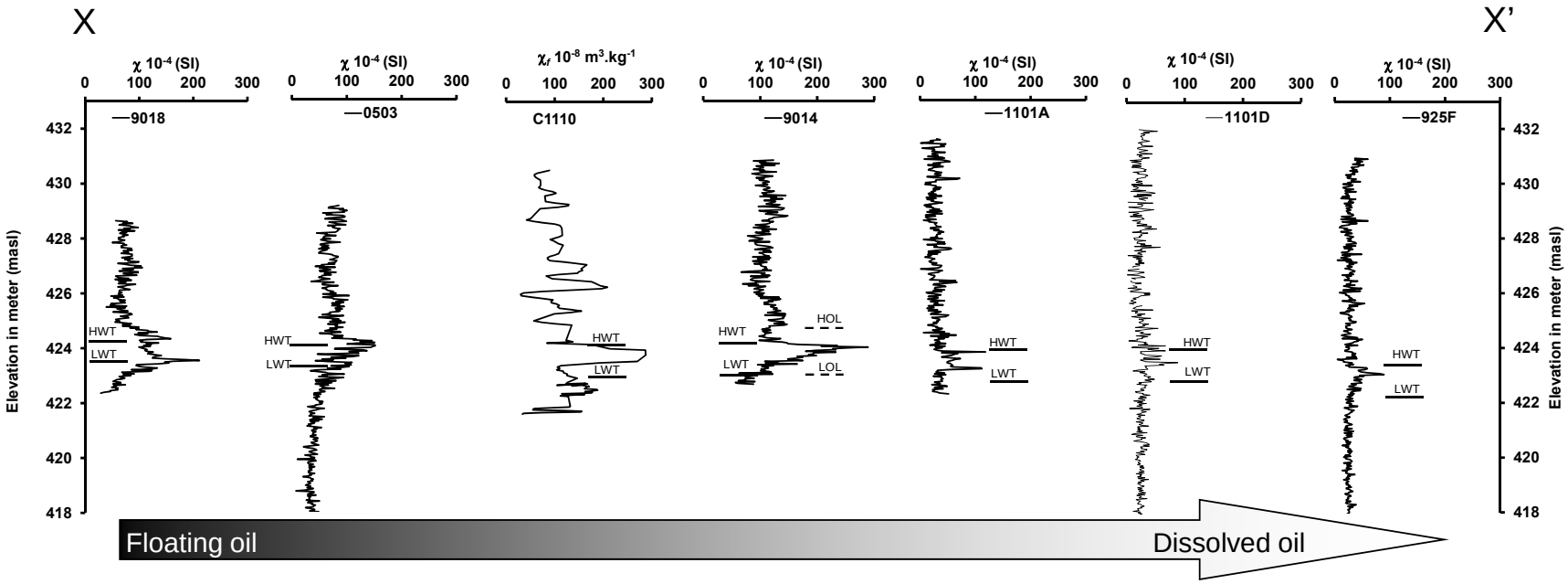

Figure 3: Magnetic susceptibility (dimensionless) profile along transect X-X' from the floating oil plume to dissolved oil plume. Highest water table (HWT), lowest water table (LWT), highest oil level (HOL) and lowest oil level (LOL) between 2000-2009 are shown. C1110 is a mass magnetic susceptibility from laboratory measurements with lower resolution. Note the decrease in the amplitude and width of the anomaly from the floating oil plume to dissolved oil plume.

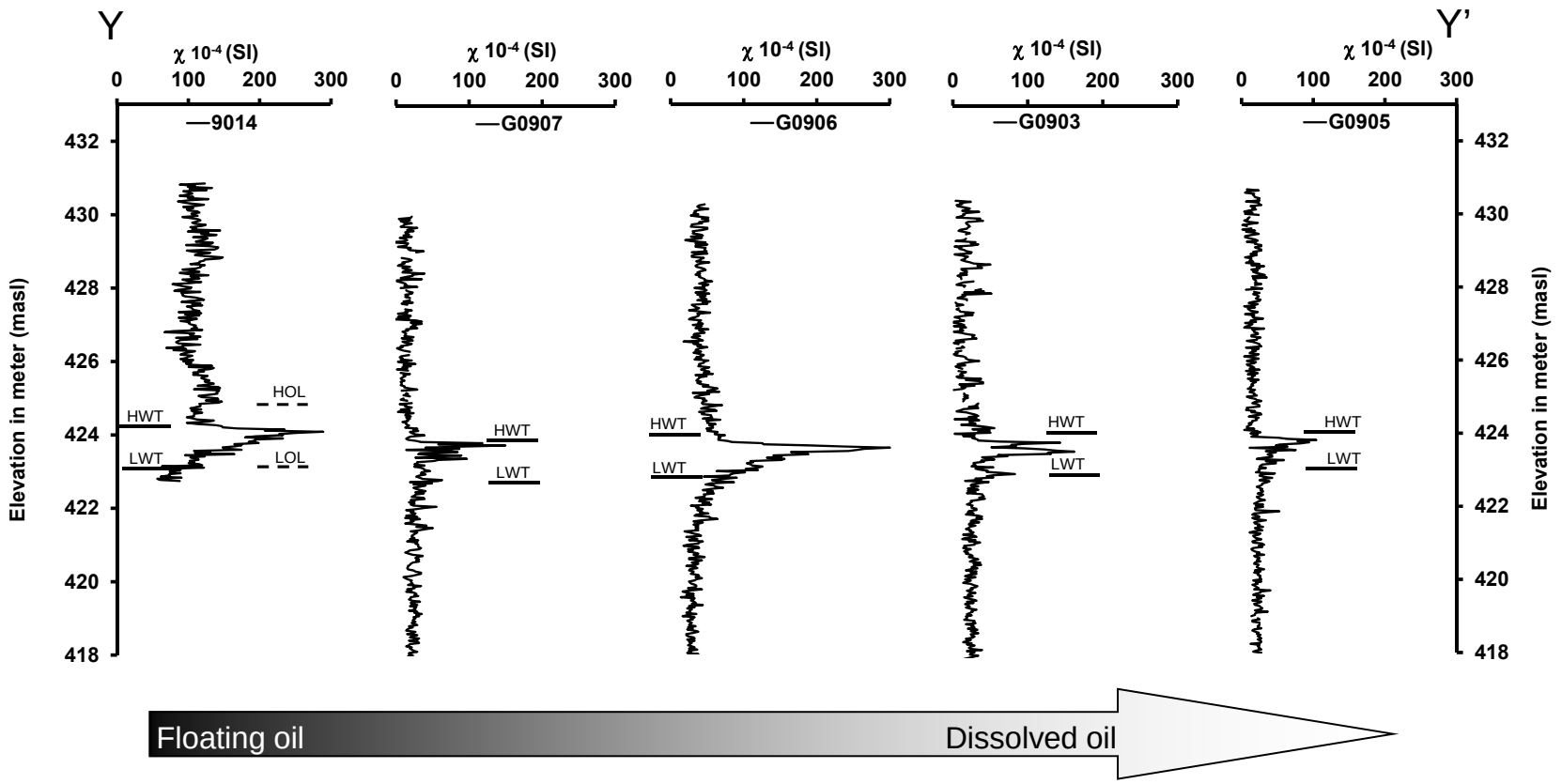

Figure 4: Magnetic susceptibility (dimensionless) profile along Y-Y' from the floating oil plume to dissolved oil plume. Highest water table (HWT), lowest water table (LWT), highest oil level (HOL) and lowest oil level (LOL) fluctuations between 2000-2009 are shown.

times higher (90 to 140×10^{-4} SI) for the free phase plume (9018, 503, 9014 and G0906) compared to ($31\text{-}43\times10^{-4}$SI) the dissolved plume (1101A, 1101D, G0905, G0903, see Figure 5 a,b).

4.5.3. Zone below WT fluctuation

The zone below the WT fluctuation shows some slightly, probably not significant, enhancement in MS values. This enhancement is higher in magnitude towards the WT (~95×10^{-4} at 422.9 masl for borehole 0503 and decreases with depth from the WT (~46.5×10^{-4} at 420 masl for borehole 0503). Also, this MS zone is higher in magnitude for the free phase plume (~46.5×10^{-4} at 420 masl for borehole 0503) compared to the dissolved phase plume (~26×10^{-4} at 420 masl for borehole 1101D).

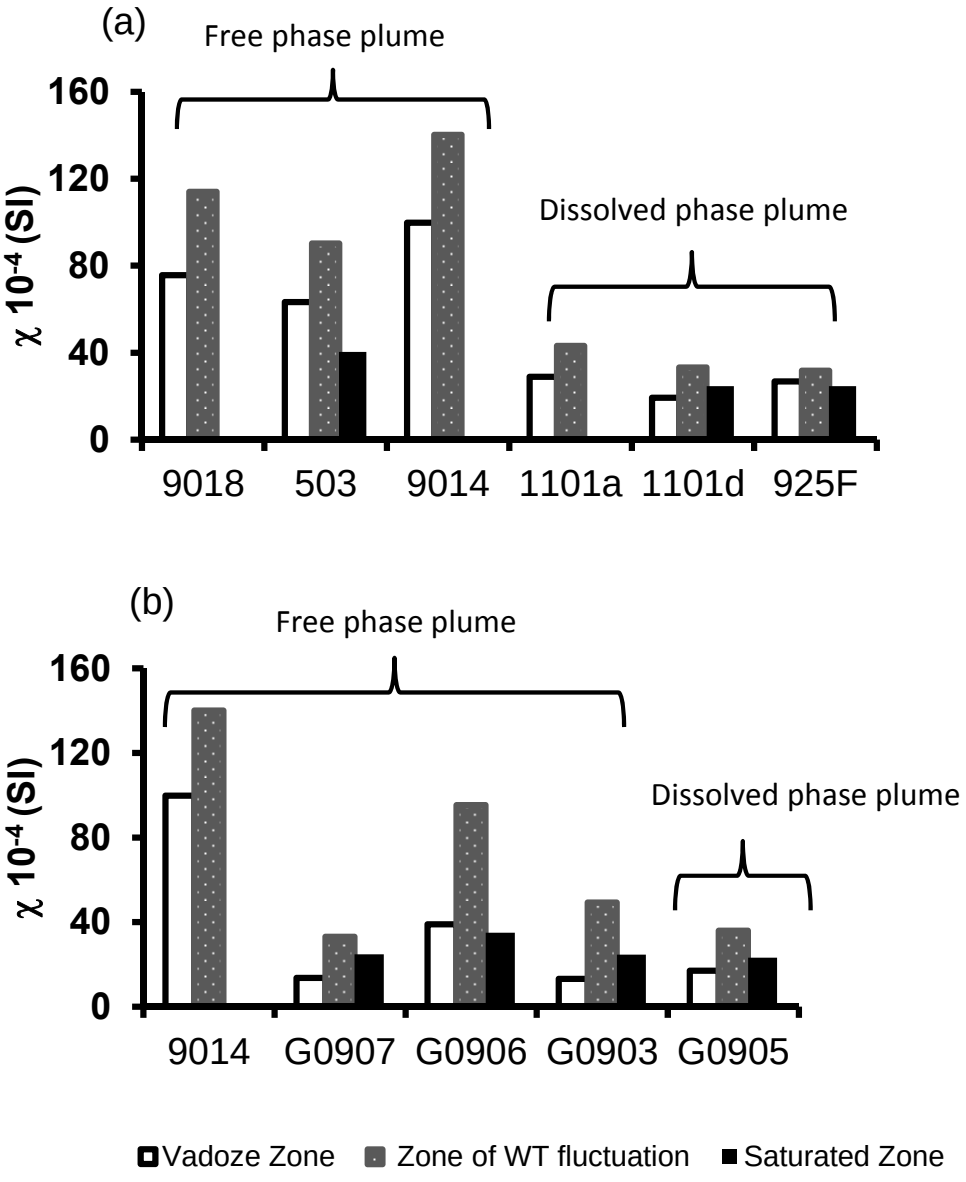

Figure 5: Histograms for the average MS values (dimensionless) for the vadose zone, the zone of water table fluctuation, and the saturated zone along (a) X-X′ and (b) Y-Y′ transects. Notice the high MS magnitude for locations within the free product compared to the dissolved product for both vadose zone and the zone of water table fluctuation.

4.6. DISCUSSION

4.6.1. Magnetic Mineral Phases

The variability in MS values, both vertically and laterally, is clearly related to the presence of hydrocarbon contamination (Figure 6) as well as the geochemical zones shown in Figure 2. For microbes to degrade oil aerobically or anaerobically, the reduction of an electron acceptor is required (Schink, 2005). When aromatic hydrocarbon oxidation is coupled to iron-reduction, it results in the reduction of ferrihydrite to iron(II) (Anderson and Lovley, 2000; Lovley et al., 1989). This process can lead to the formation of a variety of ferrous biominerals. Previous studies at the site documented the depletion of ferrihydrite towards the center of the plume with the enrichment of siderite, magnetite, and ferroan calcite (Baedecker et al., 1993; Tuccillo et al., 1999; Zachara et al., 2004). Therefore, the high MS layer observed at the contaminated locations results from the biomineralizaion of different iron mineral phases related to the oxidation of the hydrocarbons. Such high value of the magnetic susceptibility serves as an indication of the coupling of the carbon and iron biogeochemical cycles.

For the different iron mineral phases suggested across the site by previous studies (Baedecker et al., 1992; Tuccillo et al., 1999; Zachara et al., 2004), magnetite is the only iron phase that has high positive MS values as magnetite (513-1116$\times 10^{-6}$ m^3 Kg^{-1}) is a ferrimagnetic material (Dearing, 1994). In contrast, iron carbonates such as siderite

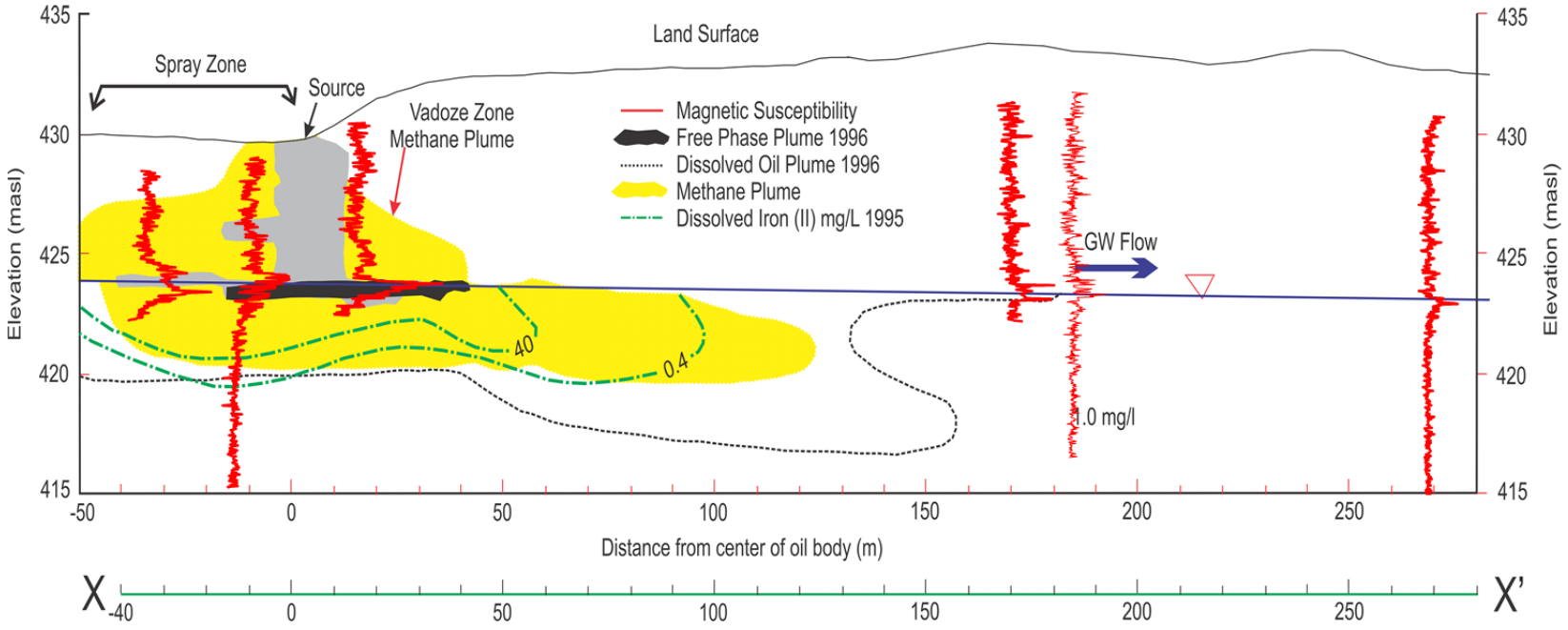

Figure 6: Magnetic susceptibility profiles superimposed on the free phase, methane and dissolved plumes and dissolved iron (II) along transect X-X' modified from the USGS [*Cozzarelli et al.*, 2001].

(1.0×10^{-6} m^3 Kg^{-1}) is antiferromagnetic materials with very low MS values (Dearing, 1994; Jacobs, 1963). In a previous study at the Bemidji site Mewafy et al. (2011), we found that the main mineral phase responsible for the high value of the magnetic susceptibility is most likely to be magnetite. The measurements of the iron weight percent (wt %) in the uncontaminated location showed no anomalous concentrations with values ranging from 0.07 to 0.22 and an average value of 0.14 wt %. In contrast, the contaminated location showed elevated values between 0.19 to 0.44 wt%. X-ray diffraction (XRD) analyses of the separated iron mineral phases suggested that siderite,

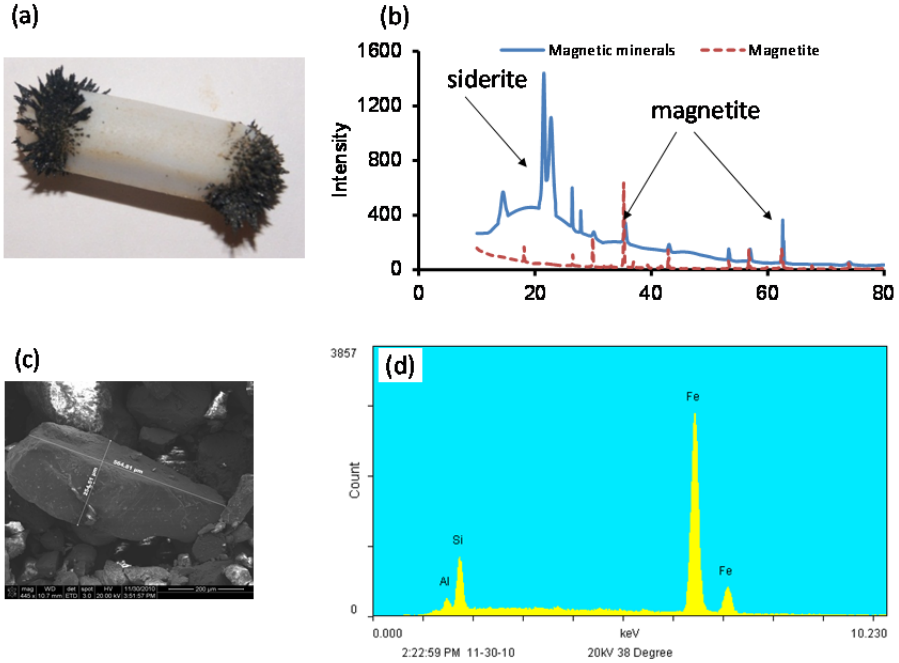

Figure 7: (a) Iron minerals separated from the sediments using a magnet bar, (b) XRD for a pure magnetite as a reference versus the XRD for the iron materials that show mainly magnetite and siderite, (C) ESEM image of the iron materials show euhedral grains, and (d) EDS analysis for the iron material shows that the majority is Fe with some silica.

magnetite and some amorphous iron mineral phase were the dominant solid mineral phases within the zone of enriched MS (Figure 7). Additionally, environmental scanning electron microscope (ESEM) imaging of the magnetic minerals using a FEI Quanta 600F SEM/EDS showed euhedral sand grains with a size range of 50µm-500µm. Energy-

dispersive X-ray spectroscopy (EDS) analyses suggested mostly Fe coatings on the sand grains.

Baedecker et al. (1992) documented the presence of magnetite and ferroan calcite within the anoxic plume and suggested that the magnetite is of authigenic origin. Also, Tuccillo et al. (1999) documented that magnetite was abundant in the ferromagnetic fraction of the bulk sediment and represents roughly 0.5% of the bulk sediment (consistent with our own results) in addition to siderite and ferroan calcite. Nonetheless, a study by Zachara et al. (2004) at the site suggested ferroan calcite precipitation and refuted the claim made by Baedecker et al. (1992) that the magnetite present in the Bemidji aquifer was of biogenic origin. Instead, using the euhedral morphology of magnetite grains, Zachara et al. (2004) suggested that the magnetite present in the Bemidji aquifer was detrital magnetite of magmatic or metamorphic origin. In this study our MS observations point to the authigenic origin of the magnetite. Figures 3-5 demonstrates that MS values are highest within the contaminated locations (especially within the free phase plume). This enrichment in magnetite across the plume is not observed for the background locations. The ESEM and EDS results show that magnetite is merely coating the sand grains. Using the grain size and/or grain shape to predict the origin of magnetite may be not always valid because the magnetite coating conforms to morphology of the sand grains. This finding supports the idea of the authigenic origin of magnetite cross the contaminated plume.

4.6.2. Fe(II) Concentration Control on MS variability

Tuccillo et al. (1999) and Amos et al. (2012) have documented reduced levels of Fe(III) in the sediments closest to and underneath the oil body (zone 3) whereas iron(II) values under the oil body (19.2 μmol/g) are as much as 4 times higher than those in the background sediments (4.6 μmol/g) (zone 1). Figure 6 shows that the dissolved Fe(II) concentrations are highest within the free phase oil plume (~ 7.1 mmol/L) within the upper parts of zone 3 and lower parts of zone 8 compared to the dissolved phase plume (less than 0.07 mmol/L; zone 4 and 5). Iron data by Bekins et al. (2001) suggests that Fe(II) builds up in excess of Fe(III) near the WT in the oil body (zone 3). Moreover, the reduction in permeability towards the WT can reduce the Fe(II) flow rate, which can increase the chance of Fe(II) complexation by organic matter (Bekins et al., 2001). Electron mass balance calculations within the Bemidji aquifer by Amos et al. (2012) suggest that CH_4 oxidation may be coupled to Fe(III) reduction. In this scenario, CH_4 oxidation linked to Fe(III) reduction within the anaerobic CH_4 plume at the Bemidji site would contribute to the release of Fe(II) and therefore the very high concentrations of Fe(II) within the methanogenic zone.

To evaluate the role of Fe(II) in the formation of the magnetic mineral phases, we superimposed the MS profiles on the Fe(II) concentrations measured in the aquifer (Figure 6). We observe that the enhancement in the MS values occur within the zone of highest Fe(II) concentration (>7.1 mmol/L) within zone 3, compared to lower MS values downgradient (<0.7 mmol/L). As predicted by Hansel et al. (2003, 2005), magnetite accumulation should only be observed at concentrations exceeding 0.3 mmol/L (equivalent to 0.5 mmol Fe(II)/g ferrihydrite), which is consistent with our MS observations and iron mineral quantification. Hansel et al. (2003) further report that

lower initial Fe(II) concentrations followed by higher concentrations promote goethite accumulation while inhibiting magnetite precipitation even when Fe(II) concentrations increase later on. Thus, the presence of higher concentrations of magnetite in zone 3 suggests higher initial concentrations and supply rates of Fe (II) within the oil plume. In addition, Zachara et al. (2002) suggest that the precipitation of magnetite typically occurs at medium supply rate and siderite at higher supply rates. The XRD results in Figure 7 document the presence of both magnetite and siderite (Mewafy et al., 2011). Therefore the intrusive or non-intrusive measurements of the magnetic susceptibility may provide important insights into the biogeochemical controls and the kinetics and mechanisms of magnetite formation and other iron mineral phases.

4.6.3. Organic Carbon Concentration control on MS Variability

Figure 6 shows high magnetic susceptibility values within the free phase plume that decreases in magnitude towards the dissolved plume. The high MS within the free phase plume is only limited to the upper parts of zone 3 and lower parts of zone 8 (Figures 2 & 6) where we have the highest concentrations of hydrocarbons including free phase oil and CH_4. The coincidence between the zone of MS enhancement and the high concentrations of hydrocarbons suggests the coupling of organic carbon oxidation with iron-reduction. It also indicates a relationship between the hydrocarbon content and the concentration of Fe(II). Zachara et al. (2002) observed in experiments on microbial iron-reduction that, when an electron donor, which is hydrocarbon in our case, was in excess, the ferrihydrite was almost fully transformed to fine-grained magnetite. This process may be similar to the situation near the oil body. Also, Rijal et al. (2012) indicated a reasonable relationship

between the mass of total non-polar hydrocarbon (TNPH) and the MS enhancement in soils.

Organic carbon content may also account for the variability in MS within the vadose zone across the site. In Figure 3 and 4, the MS in the vadose zone above the free product plume (geochemical zones 7 and 8 in Figure 2) is enhanced in contrast to that above the dissolved plume (geochemical zone 6 in Figure 2). Figure 6 shows that the MS enhancement is limited to the zone of the methane plume in the vadose zone. In a previous study (Mewafy et al., 2011), we documented that the enhancement in the MS values above the free phase plume occurred within a zone where CH_4 depletion was occurring and suggested that the formation of magnetic mineral phases provided evidence for the coupling of methane oxidation with iron-reduction consistent with recent findings reported for the saturated zone by Amos et al (2012).

4.6.4. WT fluctuations control on MS enhancement

Data along borehole 533D (see Figure 1 for location) shows fluctuations in the WT of about 1.3 meters between 422.9 and 424.2 meters above mean sea level for the period between 1989 and 2009 (Figure 8). A significant observation in this study is the fact that the enhanced MS layer occurs entirely within the highest and lowest water mark (Figures 3 and 4), suggesting that WT fluctuations have a strong control on biogeochemical processes resulting in iron mineral transformation. Similar observations have been made by Rijal et al. (2010) during a bioremediation experiment at a hydrocarbon contaminated site in Germany. They retrieved core samples from three locations. Two of the cores (S1, S2) were directly affected by groundwater fluctuations during the remediation process, while the third (S3) was less affected. They observed a more than 5 fold increase in the

magnetic parameters within the zone of WT fluctuation in cores S1 and S2, while this trend was much weaker in S3. They suggested that the zone of water table fluctuation was most biologically active and resulted in a zone of enhanced MS.

The WT interface can provide large redox gradients between highly reducing conditions below the WT and oxidizing conditions above the WT. Fluctuations in the WT may result in large temporal variations in redox conditions (Vorenhout et al., 2004). Rainwater et al. (1993) investigated the effect of WT movement on diesel-degradation in a soil column versus a static control soil column. They observed that the column subjected to WT movement had 15% less residual diesel than the static control soil column after 9 weeks. A laboratory investigation by Dobson et al. (2007) showed that WT fluctuation resulted in the entrapment of light nonaqueous-phase liquid and air below the WT and thus enhanced biodegradation. Lee et al. (2001) documented seasonal variations in the concentrations of the contaminant and byproducts in soil gas and ground water of a shallow contaminated aquifer in Korea. They indicated more active biodegradation in summer than in winter and they related this variation to WT fluctuations.

In a recent study, Rezanezhad et al. (2013) investigated the effect of WT fluctuation on soil biogeochemical processes. In one soil column, the WT remained stationary at -20 cm below the soil surface, while in the other, the WT oscillated between the soil surface and the bottom of the column. They observed dramatic changes in the redox potentials for the column with oscillating WT between ~700mV and -100mV. Interestingly, they found that WT fluctuation resulted in faster depletion of soil organic carbon. Interestingly, within the mid-section (transition zone) of the fluctuating water table

column, transient redox conditions enhanced microbial oxidation of soil organic matter, resulting in the enhanced depletion of available organic matter hence limiting the respiration rate observed at the end of the experiment. Incidentally, the authors also documented that the potential CO_2 production rates are highest in the zone with ~ 60% moisture content. They suggested that the periodic variations, together with a water saturation level on the order of 60%, resulted in the enhancement of organic carbon mineralization in the transition zone of the fluctuating column and thus enhanced the soil carbon turnover. However, the dryer and wetter conditions prevailing in the upper and lower sections of the column respectively may be limiting CO_2 production.

For the Bemidji site, the limitation of the MS enhancement layer to the zone of WT fluctuation suggests the same scenario. Sharp redox gradients occur near the water table at the Bemidji site. We suggest that WT fluctuations caused periodic variations in the redox gradients enhancing organic carbon mineralization. This process would result in high Fe(II) supply rates and therefore the formation of siderite and magnetite as predicted by the Hansel et al. (2003;2005) studies. Most of the MS anomalies, as for wells 9014, G0907, G0906, and G0905, show a gradual increase towards the WT interface with sudden decrease above the WT interface (Figure 4). This shape has been observed by Rijal et al. (2010) where they mentioned that the water resides less time at higher levels and thus flushes the hydrocarbon to lower levels. Here, we suggest that the WT fluctuation at Bemidji enhanced the biodegradation where Cozzarelli et al.,(1994) observed higher concentrations of organic ligands near the oil. This excess in organic ligands can facilitate chelation of iron from solid Fe(III) phases (Lovley et al., 1994). Also, Hansel et al., (2003) Sumoondur et al., (2008) showed in controlled experiments

that the organic ligands facilitate the precipitation of iron hydroxides such as magnetite, lepidocrocite, goethite and green rust. Moreover, the reduction in permeability towards the WT (Bekins et al., 2001) can reduce flux rate of groundwater which can help complexation of Fe(II) by organic matter. Additionally, as the iron reduction occurs in the vadose zone, this would produce Fe(II), some of which would migrate downward to the WT. Some of this Fe(II) might accumulate near the water table relative reduction in the permeability of water due to floating oil so transport of Fe(II) with the groundwater flow might be slow through the oil.

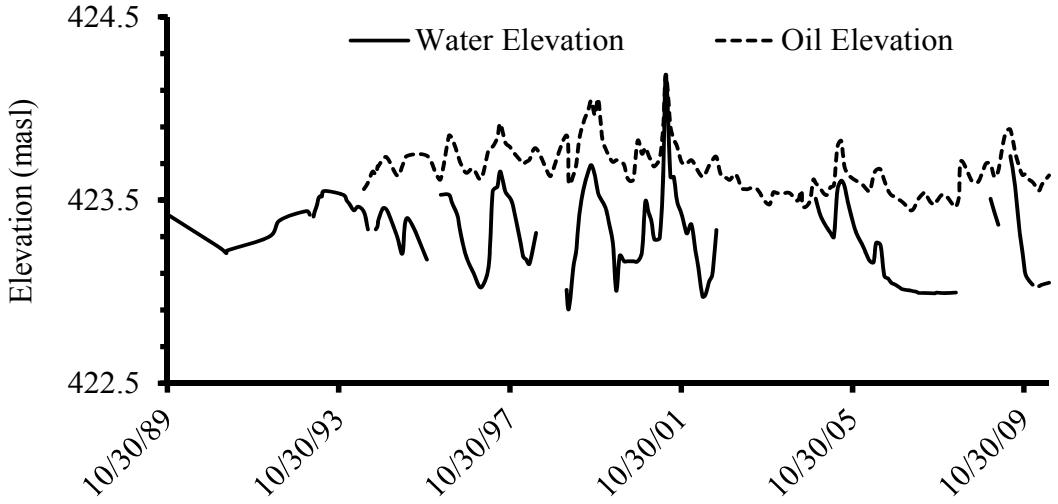

Figure 8: Oil and water table fluctuation for 1989-2009 for borehole 533D (USGS) that can result in enhancing the microbial activity within the zone of fluctuation.

Previous biogeophysical studies have pointed out that the WT interface is the most biogeochemical active zone (Abdel Aal et al., 2006; Allen et al., 2007; Atekwana et al., 2004; Werkema et al., 2003). In the above studies a clear enhancement in bulk electrical conductivity and complex conductivity was observed to have occurred within this zone. This suggest to us that biogeophysical studies can play a critical role in

delineating zones of enhanced biogeochemical processes so that they can be better studied by microbial and geochemical investigations.

4.7. CONCLUSIONS

We investigated variations in MS across an oil contaminated site undergoing active biodegradation with iron reduction and methananogenesis as the dominant biogeochemical processes occurring in the aquifer. Our results show the following: (1) The presence of an enhanced zone of magnetic susceptibility which is most likely related to magnetite enrichment within the zone of water table fluctuation. Such anomalous magnetic susceptibilities are not observed at the background locations; (2) MS values within the free product plume are higher compared to values within the dissolved product plume; (3) MS values in the vadose zone above the free product plume where methane oxidation is taking place are higher compared to vadose zone samples above the dissolved product plume; (4) High MS values (90 to 140×10^{-4} SI) coincide with zones of elevated Fe (II) concentrations limited to the upper parts of the water table; and (5) siderite and magnetite were the dominant iron biominerals but with magnetite dominating the MS response.

We suggest that under high organic carbon loading conditions, a fluctuating water table regime and fluctuating redox conditions accelerate microbial activity, hence organic carbon degradation resulting in high rates of Fe(II) production favoring the precipitation of siderite and magnetite. In contrast to previous studies that suggested the detrital origin of magnetite at this site based on the grain size and morphology, we suggest that the

magnetite enrichment within the contaminated zones supports the authigenic origin of magnetite across the site.

We conclude that MS measurements are: (1) a low cost, rapid monitoring tool for assessing the extent of hydrocarbon contamination and (2) able to delineate zones where magnetic mineral formation is occurring and serve as a proxy for regions where carbon cycling is linked to iron cycling.

4.8. REFERENCES

Abdel Aal, G. Z., L. D. Slater, and E. A. Atekwana (2006), Induced-polarization measurements on unconsolidated sediments from a site of active hydrocarbon biodegradation, *Geophysics*, *71*(2), H13-H24.

Allen, J. P., E. A. Atekwana, J. W. Duris, D. D. Werkema, and S. Rossbach (2007), The microbial community structure in petroleum-contaminated sediments corresponds to geophysical signatures, *Applied and Environmental Microbiology*, *73*(9), 2860-2870.

Amos, R., B. Bekins, I. Cozzarelli, M. Voytek, J. Kirshtein, E. Jones, and D. Blowes (2012), Evidence for iron-mediated anaerobic methane oxidation in a crude oil-contaminated aquifer, *Geobiology*.

Anderson, R. T., and D. R. Lovley (2000), Anaerobic Bioremediation of Benzene under Sulfate-Reducing Conditions in a Petroleum-Contaminated Aquifer, *Environmental Science & Technology*, *34*(11), 2261-2266.

Atekwana, E. A., E. Atekwana, F. D. Legall, and R. V. Krishnamurthy (2004), Field evidence for geophysical detection of subsurface zones of enhanced microbial activity, *Geophysical Research Letters*, *31*(23).

Baedecker, M. J., I.M. Cozzarelli, J.R. Evans, and P. P. Hearn (1992), Authigenic mineral formation in aquifers rich in organic material, *7th International Symposium on Water-Rock Interaction, Proc., A.A. Balkema*, 257–261.

Baedecker, M. J., I. M. Cozzarelli, R. P. Eganhouse, D. I. Siegel, and P. C. Bennett (1993), Crude-oil in a shallow sand and gravel aquifer .3. Biogeochemical reactions and mass-balance modeling in anoxic groundwater, *Applied Geochemistry*, *8*(6), 569-586.

Bekins, B. A., I. M. Cozzarelli, E. M. Godsy, E. Warren, H. I. Essaid, and M. E. Tuccillo (2001), Progression of natural attenuation processes at a crude oil spill site: II. Controls on spatial distribution of microbial populations, *Journal of Contaminant Hydrology*, *53*(3-4), 387-406.

Bennett, P. C., D. E. Siegel, M. J. Baedecker, and M. F. Hult (1993), Crude-oil in a shallow sand and gravel aquifer .1. Hydrogeology and inorganic geochemistry, *Applied Geochemistry*, *8*(6), 529-549.

Chaudhuri, S. K., J. G. Lack, and J. D. Coates (2001), Biogenic Magnetite Formation through Anaerobic Biooxidation of Fe(II), *Applied and Environmental Microbiology*, *67*(6), 2844-2848.

Cozzarelli, I. M., M. J. Baedecker, R. P. Eganhouse, and D. F. Goerlitz (1994), The geochemical evolution of low-molecular-weight organic-acids derived from the degradation of petroleum contaminants in groundwater

Geochimica Et Cosmochimica Acta, *58*(2), 863-877.

Cozzarelli, I. M., B. A. Bekins, R. P. Eganhouse, E. Warren, and H. I. Essaid (2010), In situ measurements of volatile aromatic hydrocarbon biodegradation rates in groundwater, *Journal of Contaminant Hydrology*, *111*(1-4), 48-64.

Cozzarelli, I. M., B. A. Bekins, M. J. Baedecker, G. R. Aiken, R. P. Eganhouse, and M. E. Tuccillo (2001), Progression of natural attenuation processes at a crude-oil spill site: 1. Geochemical evolution of the plume, *Journal of Contaminant Hydrology*, *53*(3-4), 369-385.

Dearing, J. (1994), Environmental magnetic susceptibility, *Using the Bartington MS2 system. Kenilworth, Chi Publ*.

Delin, G. N., H.I. Essaid, I.M. Cozzarelli, M.H. Lahvis, and B. A. Bekins (1998), Ground water contamination by crude oil near Bemidji, Minnesota, . *U.S. Geological Survey Fact Sheet FS*, 84–98.

Dobson, R., M. H. Schroth, and J. Zeyer (2007), Effect of water-table fluctuation on dissolution and biodegradation of a multi-component, light nonaqueous-phase liquid, *Journal of Contaminant Hydrology*, *94*(3–4), 235-248.

Dunlop, D. J., and Ö. Özdemir (2001), *Rock magnetism: fundamentals and frontiers*, Cambridge University Press.

Eganhouse, R. P., M. J. Baedecker, I. M. Cozzarelli, G. R. Aiken, K. A. Thorn, and T. F. Dorsey (1993), Crude oil in a shalloew sand and gravel aquifer.2. Organic geochemistry, *Applied Geochemistry*, *8*(6), 551-567.

Essaid, H. I., B. A. Bekins, W. N. Herkelrath, and G. N. Delin (2011), Crude Oil at the Bemidji Site: 25 Years of Monitoring, Modeling, and Understanding, *Ground Water*, *49*(5), 706-726.

Fredrickson, J. K., J. M. Zachara, D. W. Kennedy, H. L. Dong, T. C. Onstott, N. W. Hinman, and S. M. Li (1998), Biogenic iron mineralization accompanying the dissimilatory reduction of hydrous ferric oxide by a groundwater bacterium, *Geochimica Et Cosmochimica Acta*, *62*(19-20), 3239-3257.

Hansel, C. M., S. G. Benner, and S. Fendorf (2005), Competing Fe(II)-induced mineralization pathways of ferrihydrite, *Environmental Science & Technology*, *39*(18), 7147-7153.

Hansel, C. M., S. G. Benner, J. Neiss, A. Dohnalkova, R. K. Kukkadapu, and S. Fendorf (2003), Secondary mineralization pathways induced by dissimilatory iron reduction of ferrihydrite under advective flow, *Geochimica Et Cosmochimica Acta*, *67*(16), 2977-2992.

Jacobs, I. S. (1963), Metamagnetism of Siderite (FeCO<inf>3</inf>), *Journal of Applied Physics*, *34*(4), 1106-1107.

Lecoanet, H., F. Lévêque, and S. Segura (1999), Magnetic susceptibility in environmental applications: comparison of field probes, *Physics of the Earth and Planetary Interiors*, *115*(3–4), 191-204.

Lee, C., J. Lee, J. Cheon, and K. Lee (2001), Attenuation of Petroleum Hydrocarbons in Smear Zones: A Case Study, *Journal of Environmental Engineering*, *127*(7), 639-647.

Lovley, D. (1990), Magnetite formation during microbial dissimilatory iron reduction, *Iron biominerals*, *1990*, 151-166.

Lovley, D. R. (1993), Dissimilatory metal reduction, *Annual Review of Microbiology*, *47*, 263-290.

Lovley, D. R., J. C. Woodward, and F. H. Chapelle (1994), Stimulated anoxic biodegradation of aromatic-hydrocarbons using Fe(III) ligands, *Nature*, *370*(6485), 128-131.

Lovley, D. R., J. F. Stolz, G. L. Nord, and E. J. P. Phillips (1987), Anaerobic production of magnetite by a dissimilatory iron-reducing microorganism, *Nature*, *330*(6145), 252-254.

Lovley, D. R., M. J. Baedecker, D. J. Lonergan, I. M. Cozzarelli, E. J. P. Phillips, and D. I. Siegel (1989), Oxidation of aromatic contaminants coupled to microbial iron reduction, *Nature*, *339*(6222), 297-300.

Mewafy, F. M., E. A. Atekwana, D. D. Werkema, Jr., L. D. Slater, D. Ntarlagiannis, A. Revil, M. Skold, and G. N. Delin (2011), Magnetic susceptibility as a proxy for investigating microbially mediated iron reduction, *Geophys. Res. Lett.*, *38*(21), L21402.

Mortimer, R. J. G., and M. L. Coleman (1997), Microbial influence on the oxygen isotopic composition of diagenetic siderite, *Geochimica Et Cosmochimica Acta*, *61*(8), 1705-1711.

Nevin, K. P., D. E. Holmes, T. L. Woodard, E. S. Hinlein, D. W. Ostendorf, and D. R. Lovley (2005), Geobacter bemidjiensis sp. nov. and Geobacter psychrophilus sp. nov., two novel Fe(III)-reducing subsurface isolates, *International Journal of Systematic and Evolutionary Microbiology*, *55*(4), 1667-1674.

Parmar, N., Y. A. Gorby, T. J. Beveridge, and F. G. Ferris (2001), Formation of green rust and immobilization of nickel in response to bacterial reduction of hydrous ferric oxide, *Geomicrobiology Journal*, *18*(4), 375-385.

Porsch, K., U. Dippon, M. L. Rijal, E. Appel, and A. Kappler (2010), In-Situ Magnetic Susceptibility Measurements As a Tool to Follow Geomicrobiological Transformation of Fe Minerals, *Environmental Science & Technology*, *44*(10), 3846-3852.

Prommer, H., G. B. Davis, and D. A. Barry (1999), Geochemical changes during biodegradation of petroleum hydrocarbons: field investigations and biogeochemical modelling, *Organic Geochemistry*, *30*(6), 423-435.

Rainwater, K., M. P. Mayfield, C. Heintz, and B. J. Claborn (1993), Enhanced in situ biodegradation of diesei fuel by cyclic vertical water table movement: preliminary studies, *Water Environment Research*, *65*(6), 717-725.

Rijal, M. L., E. Appel, E. Petrovsky, and U. Blaha (2010), Change of magnetic properties due to fluctuations of hydrocarbon contaminated groundwater in unconsolidated sediments, *Environmental Pollution*, *158*(5), 1756-1762.

Rijal, M. L., K. Porsch, E. Appel, and A. Kappler (2012), Magnetic signature of hydrocarbon-contaminated soils and sediments at the former oil field Hänigsen, Germany, *Studia Geophysica Et Geodaetica*, *56*(3), 889-908.

Roberts, A. P., L. Chang, C. J. Rowan, C.-S. Horng, and F. Florindo (2011), Magnetic properties of sedimentary greigite (Fe3S4): An update, *Reviews of Geophysics*, *49*(1), n/a-n/a.

Schink, B. (2005), Principles of Anaerobic Degradation of Organic Compounds, in *Environmental Biotechnology*, edited, pp. 229-257, Wiley-VCH Verlag GmbH & Co. KGaA.

Stumm, W., and B. Sulzberger (1992), The cycling of iron in natural environments - considerations based on laboratory studies of heterogeneous redox processes, *Geochimica Et Cosmochimica Acta*, *56*(8), 3233-3257.

Sumoondur, A., S. Shaw, I. Ahmed, and L. G. Benning (2008), Green rust as a precursor for magnetite: an in situ synchrotron based study, *Mineralogical Magazine*, *72*(1), 201-204.

Tuccillo, M. E., I. M. Cozzarelli, and J. S. Herman (1999), Iron reduction in the sediments of a hydrocarbon-contaminated aquifer, *Applied Geochemistry*, *14*(5), 655-667.

Vorenhout, M., H. G. van der Geest, D. van Marum, K. Wattel, and H. J. P. Eijsackers (2004), Automated and Continuous Redox Potential Measurements in Soil, *J. Environ. Qual.*, *33*(4), 1562-1567.

Werkema, D. D., E. A. Atekwana, A. L. Endres, W. A. Sauck, and D. P. Cassidy (2003), Investigating the geoelectrical response of hydrocarbon contamination undergoing biodegradation, *Geophysical Research Letters*, *30*(12).

Zachara, J. M., R. K. Kukkadapu, J. K. Fredrickson, Y. A. Gorby, and S. C. Smith (2002), Biomineralization of poorly crystalline Fe(III) oxides by dissimilatory metal reducing bacteria (DMRB), *Geomicrobiology Journal*, *19*(2), 179-207.

Zachara, J. M., R. K. Kukkadapu, P. L. Gassman, A. Dohnalkova, J. K. Fredrickson, and T. Anderson (2004), Biogeochemical transformation of Fe minerals in a petroleum-contaminated aquifer, *Geochimica Et Cosmochimica Acta*, *68*(8), 1791-1805.

SECTION 2

GENERAL CONCLUSIONS

This work investigates the role of biomineral precipitation on the geophysical signatures at a hydrocarbon contaminated site undergoing biodegradation near Bemidji, Minnesota, USA. In this work, we acquired field and laboratory measurements utilizing magnetic susceptibility and complex conductivity geophysical techniques for uncontaminated (background) and oil contaminated locations at the site. A review of the objectives of this work, general observations, and conclusions are summarized below:

Contribution of metallic biominerals specifically magnetite to CC signatures

In this study, we acquired laboratory complex conductivity measurements along four cores retrieved from the North Pool. We found that the real (σ') and imaginary (σ'') conductivity are higher for samples from within the oil plume compared to background uncontaminated samples. We also conducted controlled experiments to test the effect of electrolytic variations, electrolytic conductivity, as well as biomineral precipitation. Controlled experiments indicated that variations in electrolytic conductivity and water content are unlikely to account for the higher σ'' observed within the smear zone. Instead, using magnetite as an example of the bio-metallic minerals in the smear zone at the site, a clear increase in the σ'' response with increasing magnetite content was observed. This

study reveals that the presence of bio-metallic mineral phases (e.g., magnetite) as well as electroactive dissolved iron(II) impact explain the increase in the complex conductivity.

Those two factors should be considered in the interpretation of complex conductivity data from oil contaminated sites undergoing intrinsic bioremediation.

Possibility of using the MS tool to investigate the biogeochemical changes related to microbial mediated iron reduction

To accomplish this objective, we acquired MS measurements along two cores; one retrieved from contaminated location and the second from background location. In addition, I quantified the iron minerals along the two cores. Also, we investigated the magnetic susceptibility variations down boreholes within contaminated (both free phase and dissolved phase) and uncontaminated locations. This field survey identified a layer of high MS within the zone of water table (WT) fluctuation and coincident with high concentration of dissolved Fe(II) and high organic carbon content suggesting that magnetic mineral precipitation is related to microbial iron-reduction coupled to oxidation of hydrocarbon compounds.

Also, a zone of high MS values within the vadose zone above the free phase plume was observed. This zone is coincident with a zone of methane depletion suggesting aerobic or anaerobic oxidation of methane coupled to iron-reduction. These findings suggest that magnetic susceptibility can serve as a proxy for intrinsic bioremediation by iron-reducing bacteria and for the application of geophysics to iron and carbon cycling studies. We conclude that WT fluctuation (smear) zone is the most biologically active zone due to changing redox conditions. The zones of enhanced MS show high CC values, therefore metallic biominerals play a role in enhancing the CC response. Geophysical methods can be used to track

biogeochemical processes occuring in the zone of WT fluctuation. Interpreting geophysical data acquired at a hydrocarbon contaminated site has to be guided by the biogeochemical data of that site.

Based on these findings, we conclude that the precipitation of biominerals (e.g., biometallic minerals) impacts the geophysical signatures (MS and CC in our case) at hydrocarbon contaminated sites. MS is a viable tool to follow the changes in magnetic minerals at hydrocarbon contaminate sites. Also we suggest that understanding the hydrogeochmical processes of any contaminated subsurface geologic media is critical and should be considered in the interpretation of geophysical data from contaminated sites.

RECOMMENDATIONS FOR FUTURE WORK

While this study has provided useful information regarding the MS and CC signatures at a hydrocarbon contaminated site, several questions have been raised and remained unanswered. Further research is recommended to answer these new questions and provide a better understanding of the MS and CC signatures at sites contaminated with organic carbon in general. As such, a list of questions that have been raised from this study and should be considered for future research are summarized below.

1. How does the CC vary with different rates of oil degradation?
2. What is the effect of iron grain size and morphology on the CC?
3. Do the different iron phases have the same effect on the CC?
4. Is this study applicable for other contaminated sites?
5. How long did it take to the microbes to change the iron phases?

6. What are the microbial species responsible for changing the iron phases within the zone of enhanced MS? and do the microbial species change due to changing redox conditions resulting from the changing water levels?

Finding answers for these questions can help improve our understanding of the biogeochemical processes at oil contaminated sites and hence help advance the technology of monitoring the fate and transport of contaminant within the subsurface. Additionally, investigating these problems can pave the way for advancing the sampling techniques for microbial ecology. This work also emphasizes the potential of biogeophyscial studies as cheap, cost-effective, non-invasive, and more accurate techniques for bioremediation and oil exploration.

VITA

Farag Mohamed Mewafy

Candidate for the Degree of

Doctor of Philosophy

Thesis: THE ROLE OF BIOMINERALS IN ENHANCING THE GEOPHYSICAL RESPONSE AT HYDROCARBON CONTAMINATED SITES

Major Field: Geology

Biographical:

Education:

Completed the requirements for the Doctor of Philosophy in Geology at Oklahoma State University, Stillwater, Oklahoma in May, 2013.

Completed the requirements for the Master of Science in Geophysics at Asyut University, Assiut/Egypt in 2007.

Completed the requirements for the Bachelor of Science in Geophysics at Asyut University, Assiut/Egypt in 2000.

Experience: Student contractor for the Environmental Protection Agency from June 2010 to May 2012 under the supervision of Dr. Dale Werkema and Dr. Estella Atekwana. Employed by the Boone Pickens school of Geology as a teaching and research assistant (Fall 2009-Fall 2012).

Professional Memberships:
American Association of Petroleum Geologists (AAPG)
Society of Exploration Geophysicists (SEG)
American Geophysical Union (AGU)
Geological Society of America (GSA)